

**STACY: 28-CM-THICK SLABS OF 10%-ENRICHED URANYL  
NITRATE SOLUTIONS REFLECTED WITH CONCRETE**

**Evaluators**

**Shouichi Watanabe  
Tsukasa Kikuchi<sup>a</sup>  
Japan Atomic Energy Research Institute**

**Internal Reviewers  
Yoshinori Miyoshi  
Toshihiro Yamamoto**

**Independent Reviewer**

**Virginia Dean  
Consultant to INEEL**

**Gilles Poullot  
CEA/IPSN/DPEA/SEC**

---

<sup>a</sup> Presently employed by Toshiba Corporation

## **STACY: 28-CM-THICK SLABS OF 10%-ENRICHED URANYL NITRATE SOLUTIONS REFLECTED WITH CONCRETE**

**IDENTIFICATION NUMBER:** LEU-SOL-THERM-018

**SPECTRA**

**KEY WORDS:** acceptable, concrete-reflected, critical experiment, homogeneous, low enriched uranium, moderated, slab, solution, STACY, thermal, uranyl nitrate

### **1.0 DETAILED DESCRIPTION**

#### **1.1 Overview of Experiments**

Six critical configurations included in this evaluation are part of a series of experiments with the Static Experiment Critical Facility (STACY) performed from 1997 to the summer of 1998 at the Nuclear Fuel Cycle Safety Engineering Research Facility (NUCEF) in the Tokai Research Establishment of the Japan Atomic Energy Research Institute (JAERI). Employing the 28-cm-thick, 69-cm-wide slab core tank, a 10%-enriched uranyl nitrate solution was used in these experiments. The uranium concentration and the free nitric-acid concentration were adjusted to approximately 310-315 g/l and 0.8-1.0 mol/l, respectively. Six thicknesses of reflectors, concrete blocks packed in slab-shaped containers, were prepared and arranged symmetrically on the large side walls of the core tank. All six experiments are acceptable benchmark experiments.

Other STACY experiments with 10%-enriched uranyl nitrate solution are evaluated in LEU-SOL-THERM-004, LEU-SOL-THERM-016, and LEU-SOL-THERM-020 (water reflector); LEU-SOL-THERM-007, LEU-SOL-THERM-017, and LEU-SOL-THERM-021 (unreflected); LEU-SOL-THERM-008 (concrete reflector), LEU-SOL-THERM-009 (borated-concrete reflector); and LEU-SOL-THERM-010 and LEU-SOL-THERM-019 (polyethylene reflector).

#### **1.2 Description of Experimental Configuration**

The schematic view of the 280T core tank is shown in Figure 1. The dimensions shown in mm units are the design values. The 280T core tank was made of stainless steel, S.S.304L (or SUS304L), and the inner-thickness, inner-width, and inner-height design values were, respectively, 280 mm, 690 mm, and 1500 mm. The side walls, lower plate, and upper plate thicknesses were respectively 25 mm, 20 mm, and 25 mm. The inspected dimensions of the 280T core tank compared with design values are listed in Table 1. The standard deviation ( $1\sigma$ ) is due to many measurements during the inspection process. The accuracy means the precision of the measurement instrument.

## LEU-SOL-THERM-018

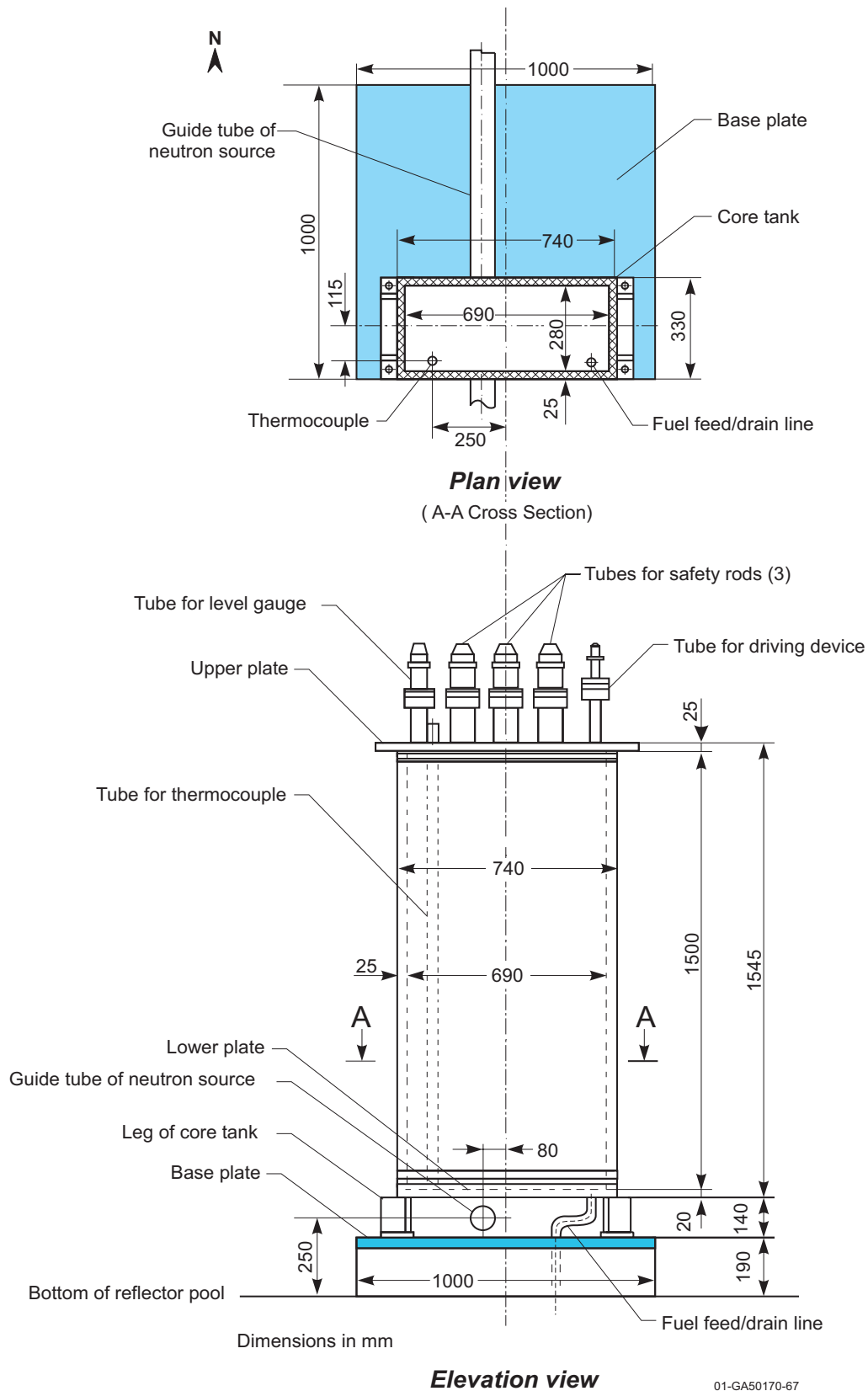


Figure 1. Schematic View of STACY Core Tank.  
( design dimensions )

Table 1.a. Dimensions of the 280T-Slab Core Tank (Unit: mm).

| Tank         | Dimension   | Inspected Result <sup>(a)</sup> | Design Value |
|--------------|-------------|---------------------------------|--------------|
| (inner size) | thickness   | 280.8±0.5                       | 280.0        |
|              | width       | 690.3±0.5                       | 690.0        |
|              | height      | 1497.5±0.6                      | 1500.0       |
| (thickness)  | side wall   | 25.3±0.1                        | 25.0         |
|              | lower plate | 20.4±0.1                        | 20.0         |
|              | upper plate | 28.8±0.1                        | 25.0         |

(a) Uncertainties are from the standard deviation of inspected data and the accuracy, added quadratically.

Table 1.b. Detailed Measurements <sup>(a)</sup> of the 280T-Slab Core Tank (Unit: mm).

| Measured Item            | Number of Measured Points | Average | Standard Deviation | Accuracy | Uncertainty |
|--------------------------|---------------------------|---------|--------------------|----------|-------------|
| Thickness of upper plate | 4                         | 28.75   | 0.03               | 0.10     | 0.10        |
| Thickness of lower plate | 14                        | 20.41   | 0.02               | 0.10     | 0.10        |
| Thickness of side wall   | 90                        | 25.32   | 0.03               | 0.10     | 0.10        |
| Outer height of tank     | 4                         | 1546.61 | 0.24               | 0.50     | 0.55        |
| Outer thickness of tank  | 45                        | 331.39  | 0.13               | 0.50     | 0.52        |
| Outer width of tank      | 30                        | 740.95  | 0.11               | 0.50     | 0.51        |

(a) The outer size of the tank is measured by the usual methods, and the others are measured by the supersonic wave-measure method.

In this paper, all measurements are given with an uncertainty corresponding to one standard deviation.

The core tank was vertically penetrated by a tube (the outer diameter was 17.3 mm, and its wall thickness was 3.2 mm) for thermocouples; this tube extended to the bottom of the core tank. A level gauge and three cylindrical safety rods containing B<sub>4</sub>C pellets were held at the upper part of the core tank. In their withdrawn position, the bottom of the safety rods was at 1850 mm above the bottom of the core tank. In their fully inserted position, the bottom of the safety rods was at 50 mm above the bottom of the core tank. The cladding tube of the safety rod, which was made of stainless steel, had an outer diameter of 61.9 mm, an inner diameter of 54.9 mm, a bottom cover thickness of 3.5 mm, and total length of 2277 mm. The diameter of the B<sub>4</sub>C pellets was 54.6 mm, and their active length in the cladding tube was 1550 mm.

The fuel solution was fed into the tank from the bottom through the fuel feed/drain line, which had an outer diameter of 27.2 mm and a thickness of 2.9 mm. In the operating condition, the fuel feed/drain line was filled with fuel solution.

The core tank was supported by four stainless steel legs. These legs were 140 mm high, and stood on the core tank support. The top of the core tank support was a stainless steel base plate, which was 1000 mm wide, 1000 mm long, and 30 mm thick. The base plate was centered under the tank in the east-west direction, but was not centered in the north-south direction, as shown in Figure 1. The base plate was supported by 160-mm-high stainless steel beams located on the bottom of the empty water-reflector pool tank. A guide tube, which had an outer diameter of 89.1 mm and a thickness of 5.5 mm, for inserting an Am-Be neutron source lay horizontally between the lower plate of the core tank and the base plate in the north-south direction. The centerline of this tube was 100 mm below the bottom of the active region in the core tank, and 80 mm west of the centerline of the core tank.

The schematic view of the configuration in which two reflectors were arranged next to each of the two larger side walls of the core tank is shown in Figure 2. The reflector material was packed in the slab-shaped containers, which consisted of the frame plates and the cover plates. The frame plates, which were made of stainless steel, surrounded the reflector material on the four small sides, and had a nominal thickness of 30 mm. The cover plates, which were made of aluminum, held the concrete and the frame plates on the two larger sides, and had a nominal thickness of 8 mm.

For the experiments, four sizes of reflectors were prepared; they were named C25, C50, C100 and C150, for which the reflector design thicknesses were 25, 50, 100 and 150mm. A dimensional inspection was carried out after fabrication. The inner gaps between the core tank and the reflectors were measured for each experiment. The experimental cases and the smaller horizontal dimensions are listed in Table 2. The larger horizontal dimensions and the vertical dimensions of each reflector are listed in Tables 3 and 4, respectively. The active size of concrete is equal to the inner size of the container, because the reflectors were built by directly packing the concrete into the containers.

To insert a small neutron detector or a gold wire, the reflectors were horizontally and/or vertically penetrated by small holes. The diameters of the holes are 16 mm for neutron detectors and 5 mm for gold wire. (Details are given in Appendix D.)

Four legs of the reflector support, which were made of stainless steel, stood on the bottom of the pool tank (south side) or the base plate (north side). The heights of these legs were 32 cm on the south side and 13 cm on the north side.

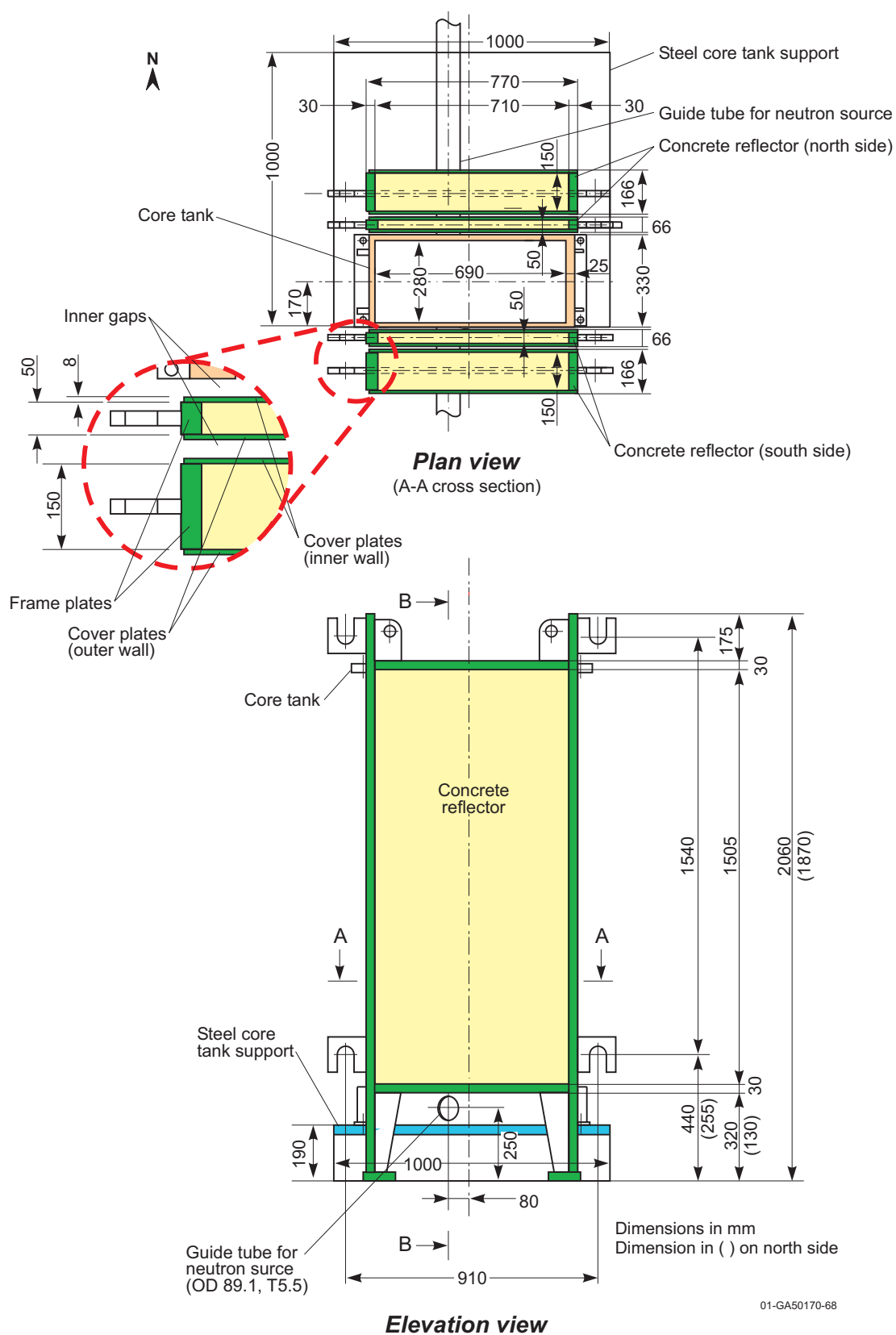


Figure 2.a. Schematic View of the Core Tank and the Reflector (C200).  
( design dimensions )

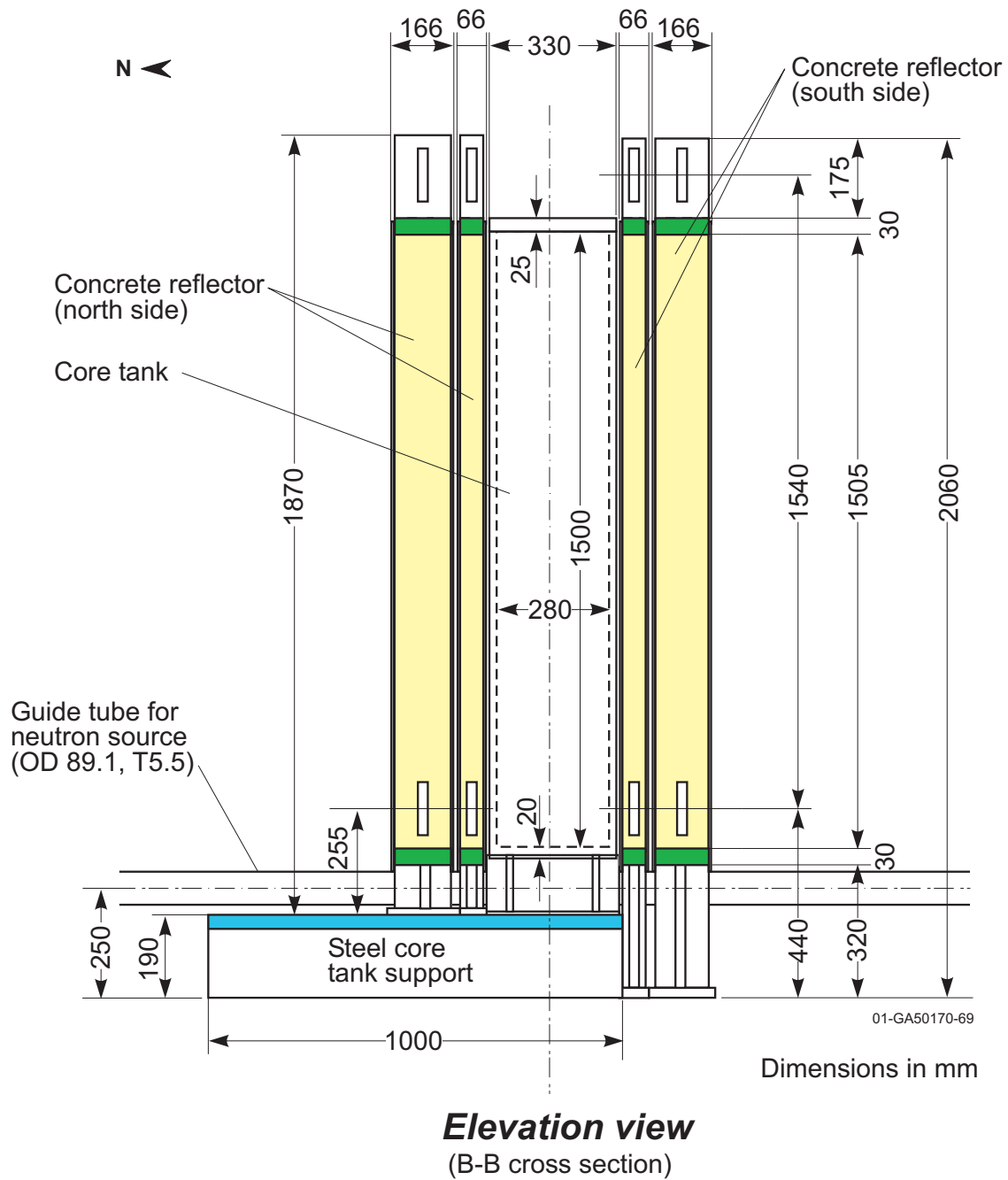


Figure 2.b. Schematic View of the Core Tank and the Reflector (B-B cross section).

Table 2. Smaller Horizontal Dimensions<sup>(a)</sup> of Reflectors (Unit : cm).

| Run No.       | Reflector | Inner Gap | Inner Wall | Concrete Region | Outer Wall |
|---------------|-----------|-----------|------------|-----------------|------------|
| 133           | C150      | 0.23±0.03 | 0.81±0.01  | 15.00±0.04      | 0.81±0.01  |
| 142           | C25       | 0.27±0.06 | 0.81±0.01  | 2.53±0.05       | 0.81±0.01  |
| 143           | C50       | 0.21±0.03 | 0.81±0.01  | 5.01±0.04       | 0.81±0.01  |
| 144           | C100      | 0.22±0.04 | 0.81±0.01  | 10.07±0.04      | 0.81±0.01  |
| 145<br>(C200) | C50       | 0.22±0.04 | 0.81±0.01  | 5.01±0.04       | 0.81±0.01  |
|               | C150      | 0.08±0.06 | 0.81±0.01  | 15.00±0.07      | 0.81±0.01  |
| 146<br>(C300) | C50       | 0.23±0.05 | 0.81±0.01  | 5.01±0.04       | 0.81±0.01  |
|               | C150      | 0.06±0.06 | 0.81±0.01  | 15.00±0.07      | 0.81±0.01  |
|               | C100      | 0.16±0.08 | 0.81±0.01  | 10.07±0.04      | 0.81±0.01  |

- (a) The dimensions are averages of the north and south side values. Two or three kinds of reflectors were combined for Run No.145 and 146. These reflectors are listed in the table in order, from the inner position next to the core tank.

Table 3. Larger Horizontal Dimensions<sup>(a)</sup> of Reflectors (Unit : cm).

| Reflector | Side  | Active Width of Concrete/<br>Inner Width of Container | Thickness<br>of Side Walls |
|-----------|-------|---|----------------------------|
| C25       | north | 71.4±0.1  | 3.02±0.01                  |
|           | south | 71.4±0.1  | 3.02±0.02                  |
| C50       | north | 71.5±0.1  | 3.01±0.02                  |
|           | south | 71.5±0.1  | 3.01±0.02                  |
| C100      | north | 71.5±0.1  | 2.99±0.01                  |
|           | south | 71.4±0.1  | 2.99±0.01                  |
| C150      | north | 71.5±0.1  | 3.02±0.01                  |
|           | south | 71.4±0.1  | 3.02±0.02                  |

- (a) The concrete was directly built in the containers, so the active width of material is equal to the inner width of the container. The thickness of side walls is the average of the east and west walls.



Table 4. Vertical Dimensions<sup>(a)</sup> of Reflectors (Unit : cm).

| Reflector | Side  | Thickness of Lower Plate | Active Height of Concrete/<br>Inner Height of Container | Thickness of Upper Wall |
|-----------|-------|--------------------------|---|-------------------------|
| C25       | north | 3.02±0.01                | 150.5±0.1   | 3.03±0.01               |
|           | south | 3.02±0.01                | 150.6±0.1   | 3.01±0.01               |
| C50       | north | 2.98±0.01                | 150.4±0.1   | 2.98±0.01               |
|           | south | 2.99±0.01                | 150.6±0.1   | 3.03±0.01               |
| C100      | north | 3.00±0.01                | 150.6±0.1   | 2.98±0.01               |
|           | south | 2.98±0.01                | 150.6±0.1   | 2.99±0.01               |
| C150      | north | 3.05±0.01                | 150.6±0.1   | 3.04±0.01               |
|           | south | 3.04±0.01                | 150.7±0.1   | 3.04±0.01               |

(a) The concrete was directly built in the containers, so the active height of the material is equal to the inner height of the container.

The scale drawing and side views of the large empty tank in which the core tank and the reflectors were set are shown in Figures 3.a and 3.b. The outer dimensions of the pool tank, which was made of stainless steel, were 2020 mm width (east-west direction), 4020 mm length (north-south direction), and 2400 mm height. The thicknesses of the side walls and of the bottom plate were 10 mm and 15 mm, respectively. The bottom of the core tank was 330 mm above the bottom of the pool tank. The shortest distance between the side wall of the core tank and the inner surface of the pool tank is approximately 630 mm. The reflector on the north side of the core tank was set on the base plate of the core tank, and the reflector on the south side of the core tank was set on the bottom of water-reflector pool, as shown in Figure 3.b. The heights of the reflector legs, which were made of stainless steel, were 130 mm for the north-side reflector and 320 mm for the south-side reflector, as shown in Figure 2. By these reflector legs, the lower ends of the reflector materials were adjusted to within 0.1 cm of the same level as the bottom of the active fuel region in the core tank.

The pool tank was surrounded by a hood. The hood had a cubic shape and its internal dimensions were 9 x 10 meters horizontally and 9.8 meters high. This hood was installed in the reactor room, which was 12.6 meters wide, 13.1 meters long, and 12.1 meters high (Figure 4). All walls of the reactor room were made of concrete. The thickness of the concrete wall was more than 1 meter.

The STACY facility consisted of the core tank containing fuel solution, a solution transfer system, a fuel treatment system, and a fuel storage system. Reactivity was controlled by adjusting the fuel solution level in the core tank. Initially, a fast-feed pump was used to feed the fuel solution to just below half of the predicted critical height. After that, a slow-feed pump was used to feed the fuel solution to the near-critical state. The maximum excess reactivity and maximum reactivity addition rate were adjusted by limiting the position of the contact-type level gauge and the feed speed of the slow-feed pump. The level gauge consisted of a needle to detect the surface of solution, an electric

motor for changing the vertical position of the needle, and an encoder indicating the vertical position. The accuracy of this level gauge was 0.2 mm.

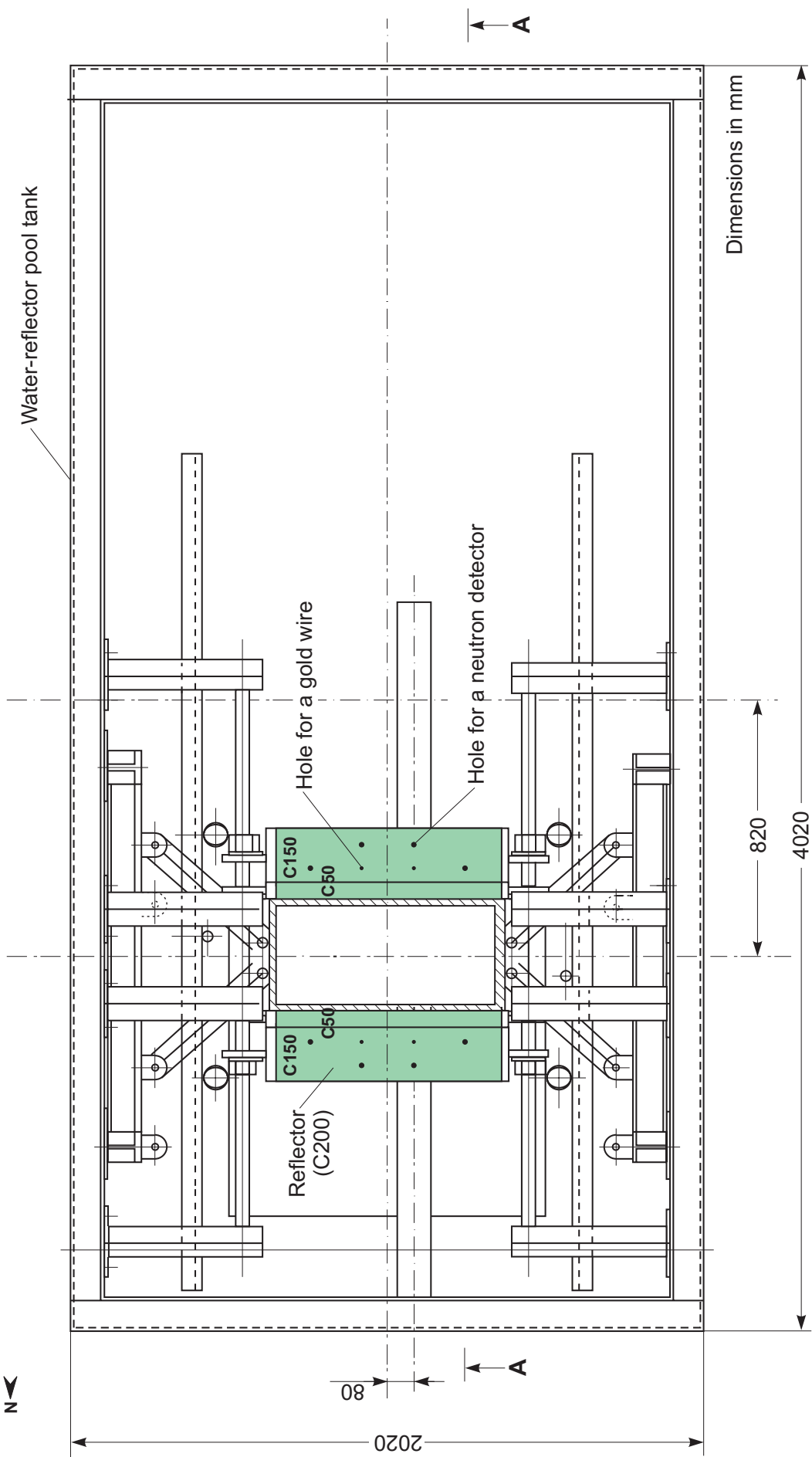
The accuracy of the level gauge (0.2 mm) was determined during the inspection at manufacture, using a highly accurate gauge as reference. The reproductive performance of this gauge, which is confirmed every annual inspection by using a higher-accuracy gauge, is almost within 0.02 mm (1/10 of the accuracy). After every annual inspection or changing the core tank, the adjustment of the zero level is performed by directly detecting the bottom of the core tank and resetting the indication of level gauge.

The bottom of the tank was exactly flat and horizontal. After manufacturing the tank, the inclination of the bottom plate was measured and found to be within 0.6 mm (maximum height minus minimum height at edge). Also, after setting the core tank in the pool tank, the inclination of the axis was measured and found to be within 1/1500 mm per mm.

To obtain the critical height, first a critical solution height was confirmed by observing the steady-state neutron flux level. Then the final critical height was determined by a series of reactivity measurements for which the fuel solution was repeatedly drained and fed near the critical state. In the measurements, subcritical and supercritical conditions were repeated, not only subcritical conditions. For example, measured reactivities might have been -3 cents, +3 cents, -6 cents, +6 cents, -9 cents, and +9 cents. The reactivities were measured, employing a digital reactivity meter. A digital reactivity meter calculates reactivities by solving the reactor kinetics equation in real time, using an analog signal from a neutron detector. Near the critical state, reactivity is linear with solution height.

The arrangement of the neutron detectors is shown in Figure 5. The positions of the neutron detectors were variable depending on the experimental requirements. Figure 5 shows the arrangement for Run No.145 as an example, in which the experiment of the symmetric reflected condition with C50 and C150 reflectors (i.e. C200 reflector) was performed. Two  $^{10}\text{B}$ -lined proportional counters (ST-A and B) and four gamma-ray compensated ionization chambers (LIN-A, B, LOG-A and B) were located around the core tank to measure the neutron flux level for the start-up power range and the operational power range, respectively. Maximum power was limited to 200W. Nine additional experimental neutron detectors were also located around the core tank: two  $^3\text{He}$  proportional counters (Ch-1 and 3) on the west side, one gamma-ray compensated ionization chamber (Ch-7), used as input to a digital reactivity meter on the west side, one  $^3\text{He}$  proportional counter (Ch-2) on the east side, one gamma-ray compensated ionization chamber (Ch-5) on the east side, one  $^3\text{He}$  proportional counter (Ch-8) on the north side, one  $^{10}\text{B}$ -lined proportional counter (Ch-4), one  $^3\text{He}$  proportional counter (Ch-9) on the south side, and one  $^3\text{He}$  proportional counter (Ch-10) in the southern reflector. Further, a pulsed neutron source (Pulsatron) was located on the north side for Run No. 144. For improving the neutron efficiency, the detectors were covered with polyethylene. The thicknesses of polyethylene are given in the tables in Figure 5.a.

Six critical conditions are summarized in Table 5.



01-GA50170-70

Figure 3.a. Horizontal View of an Experiment in the Empty Water-Reflector Pool Tank.

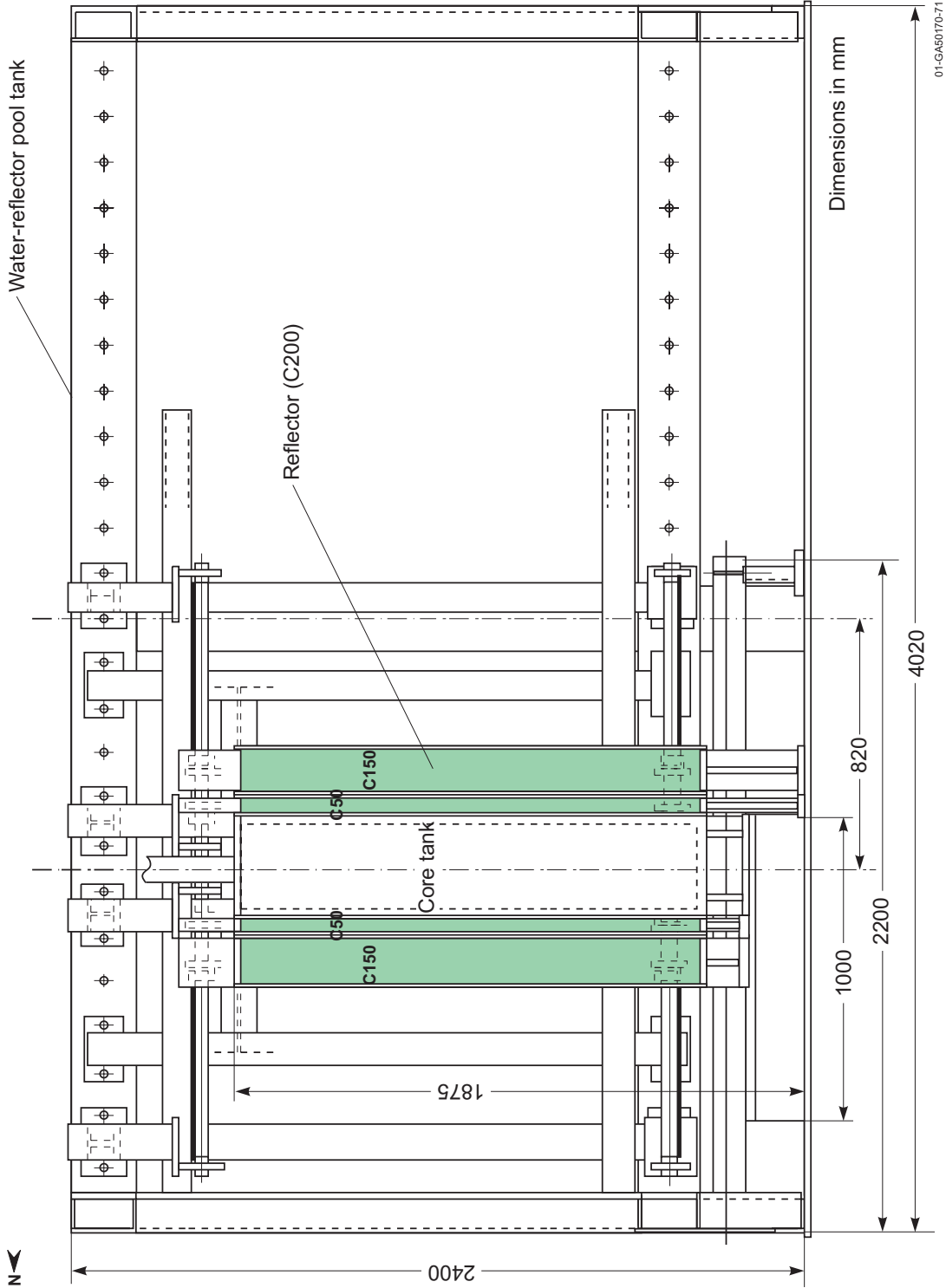


Figure 3.b. Elevation View of an Experiment in the Empty Water-Reflector Pool Tank (A-A cross section).

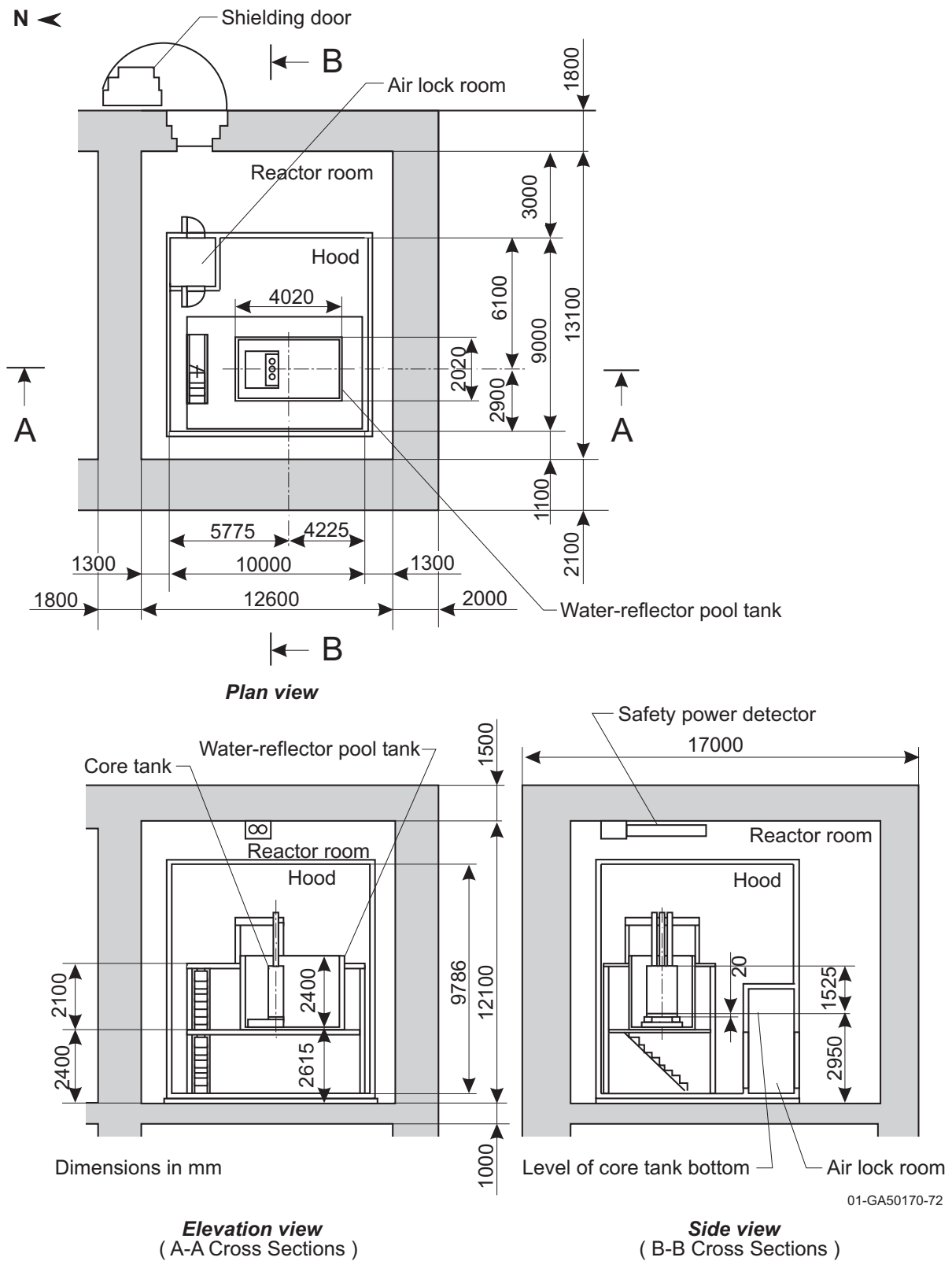
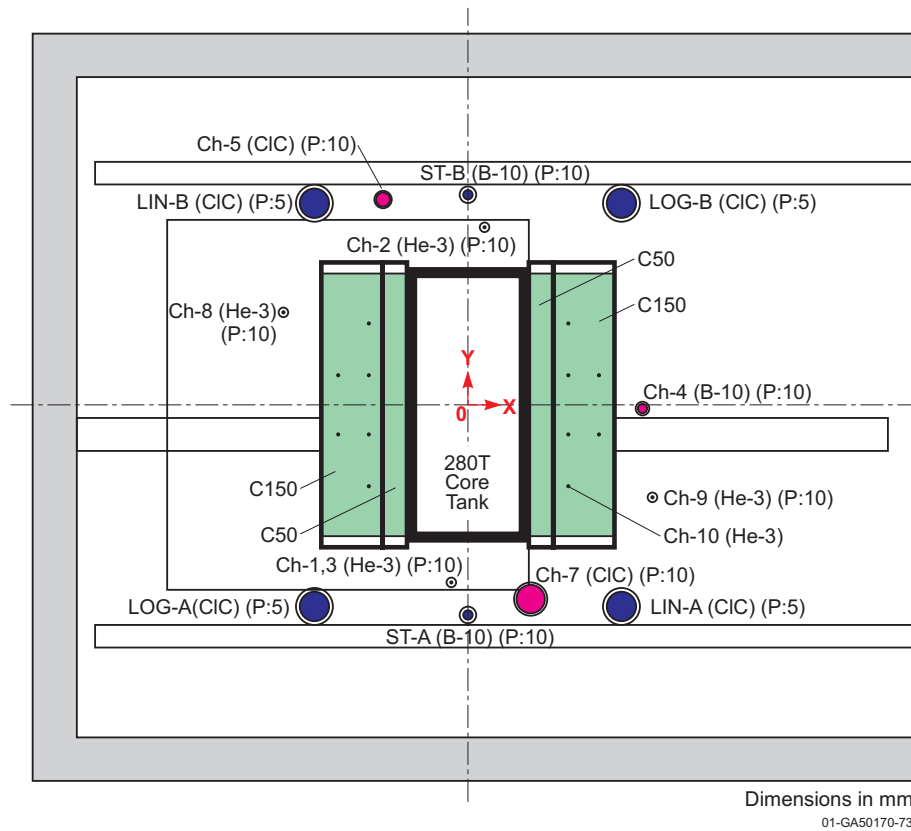


Figure 4. Schematic View Inside the Reactor Room.

LEU-SOL-THERM-018



**Experimental Channels**

| ID    | Type    | X , Y      | Hc  | OD1  | L1    | OD2  | A   | L , U (A)   | P    | L , U (P) |
|-------|---------|------------|-----|------|-------|------|-----|-------------|------|-----------|
| Ch-1  | He-3(H) | -45 , -480 | 168 | 6.0  | 82.5  | 22.0 | 1.0 | -160 , 2240 | 10.0 | 73 , 263  |
| Ch-2  | He-3(H) | 45 , 480   | 335 | 6.0  | 82.5  | 22.0 | 1.0 | -160 , 2240 | 10.0 | 240 , 430 |
| Ch-3  | He-3(H) | -45 , -480 | 503 | 6.0  | 82.5  | 22.0 | 1.0 | -160 , 2240 | 10.0 | 408 , 598 |
| Ch-4  | B-10    | 473 , -10  | 335 | 25.4 | 295.1 | 37.0 | 3.0 | 149 , 623   | 10.0 | 161 , 541 |
| Ch-5  | CIC     | -230 , 555 | 335 | 38.1 | 235.0 | 47.0 | 3.0 | 177 , 601   | 10.0 | 189 , 539 |
| Ch-7  | CIC     | 170 , -525 | 335 | 77.0 | 241.0 | 90.0 | 4.0 | 188 , 699   | 10.0 | 218 , 578 |
| Ch-8  | He-3(L) | -500 , 250 | 335 | 6.3  | 10.0  | 22.0 | 1.0 | -350 , 2050 | 10.0 | 310 , 360 |
| Ch-9  | He-3(L) | 500 , -250 | 335 | 6.3  | 10.0  | 22.0 | 1.0 | -350 , 2050 | 10.0 | 310 , 360 |
| Ch-10 | He-3(H) | 272 , -220 | 400 | 6.0  | 82.5  | -    | -   | - , -       | -    | - , -     |

**Nuclear Instruments**

| ID    | Type | X , Y       | Hc  | OD1  | L1    | OD2   | A   | L , U (A)   | P    | L , U (P) |
|-------|------|-------------|-----|------|-------|-------|-----|-------------|------|-----------|
| ST-A  | B-10 | 0 , -568    | 200 | 25.4 | 266.7 | 45.0  | 3.0 | -350 , 2150 | 10.0 | -25 , 425 |
| ST-B  | B-10 | 0 , 568     | 200 | 25.4 | 266.7 | 45.0  | 3.0 | -350 , 2150 | 10.0 | -25 , 425 |
| LIN-A | CIC  | 416 , -545  | 343 | 79.5 | 355.6 | 100.0 | 3.0 | -350 , 2150 | 5.0  | 63 , 623  |
| LIN-B | CIC  | -416 , 545  | 343 | 79.5 | 355.6 | 100.0 | 3.0 | -350 , 2150 | 5.0  | 63 , 623  |
| LOG-A | CIC  | -416 , -545 | 343 | 79.5 | 355.6 | 100.0 | 3.0 | -350 , 2150 | 5.0  | 63 , 623  |
| LOG-B | CIC  | 416 , 545   | 343 | 79.5 | 355.6 | 100.0 | 3.0 | -350 , 2150 | 5.0  | 63 , 623  |

X,Y: Horizontal position

Hc : Height of center of neutron counter relative to bottom of active core

OD1: Counter diameter

L1: Counter length

OD2: Outer diameter of aluminum guide tube and inner diameter of polyethylene sheet

A, P: Thicknesses of aluminum guide tube and polyethylene sheet, respectively

L,U (A): Height of lower and upper end of aluminum guide tube, respectively

L,U (P): Height of lower and upper end of polyethylene sheet, respectively

Origin of vertical position is the bottom of solution.

He Gas Pressure: He-3(H); 102Pa, He-3(L); 39Pa Polyethylene Density: 0.97 g/cm<sup>3</sup>

Figure 5.a. Neutron-Detector Locations, from Above (Run No. 145, C200 Reflector).

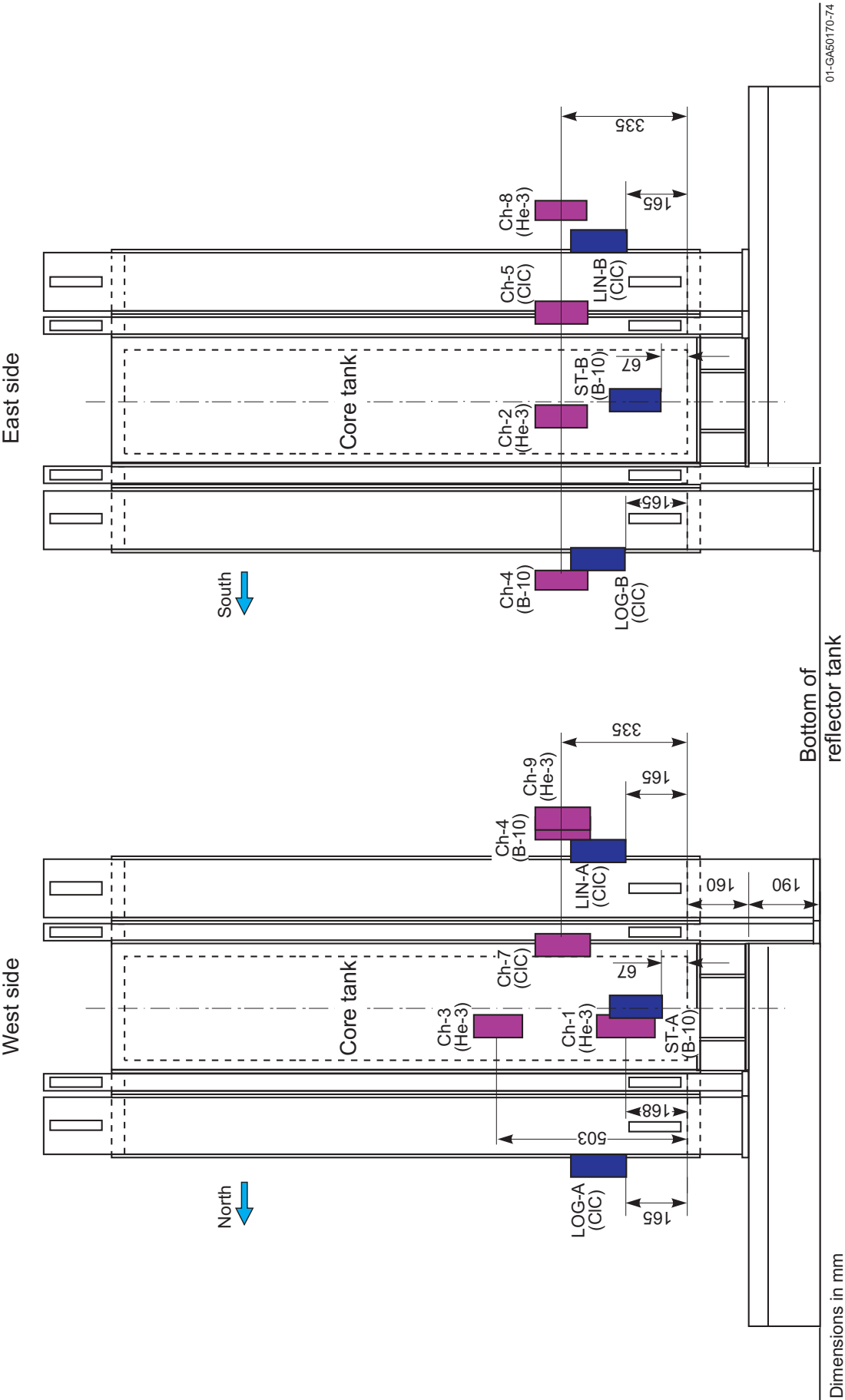


Figure 5.b. Counter Allocation from West.

Figure 5.c. Counter Allocation from East.

### 1.3 Description of Material Data

The chemical analyses (uranium concentration, free nitric acid concentration, and solution density) of the uranyl nitrate solution were carried out approximately every week during a series of experiments. The uranium concentration and the free nitric acid concentration were adjusted to approximately 310-315 gU/l and 0.8-1.0 mol/l, respectively.

The fuel solution characteristics at the time of each experiment were determined by interpolation of the chemical analyses and are given in Table 5. The uncertainties of the measured values in Table 5 include uncertainties for the interpolation.

Table 5. Critical conditions of STACY.

| Run No. | Date (yy.mm.dd) | Reflector | Condition of fuel solution at 25 °C |                        |                              | Critical Height (cm) | Temp. (°C) |
|---------|-----------------|-----------|-------------------------------------|------------------------|------------------------------|----------------------|------------|
|         |                 |           | U Conc. (gU/l)                      | H <sup>+</sup> (mol/l) | Density (g/cm <sup>3</sup> ) |                      |            |
| 133     | 97.07.22        | C150      | 308.1±0.7                           | 0.800±0.014            | 1.4380±0.0006                | 67.91±0.02           | 24.8       |
| 142     | 97.10.15        | C25       | 312.2±0.6                           | 0.955±0.015            | 1.4476±0.0005                | 80.57±0.02           | 24.9       |
| 143     | 97.10.20        | C50       | 312.7±0.6                           | 0.955±0.015            | 1.4484±0.0005                | 73.18±0.02           | 24.7       |
| 144     | 97.10.24        | C100      | 313.2±0.6                           | 0.955±0.015            | 1.4490±0.0004                | 67.95±0.02           | 25.0       |
| 145     | 97.10.30        | C200      | 313.8±0.6                           | 0.955±0.015            | 1.4500±0.0004                | 65.56±0.02           | 25.2       |
| 146     | 97.11.06        | C300      | 314.6±0.6                           | 0.955±0.015            | 1.4511±0.0004                | 65.00±0.02           | 25.2       |

The isotopic composition of uranium, which was measured by mass spectrometry before the series of experiments, is given in Table 6. The enrichment of the uranium was 9.97±0.013 wt.%.

Table 6. Isotopic Composition of Uranium.

| Isotope          | wt. %      |
|------------------|------------|
| <sup>234</sup> U | 0.08       |
| <sup>235</sup> U | 9.97±0.013 |
| <sup>236</sup> U | 0.01       |
| <sup>238</sup> U | 89.94      |

Uranyl nitrate solution consists of uranyl nitrate [UO<sub>2</sub>(NO<sub>3</sub>)<sub>2</sub>], free nitric acid [HNO<sub>3</sub>], and water [H<sub>2</sub>O]. A sample of uranyl nitrate solution was taken from the dump tank, which was located in the basement under the reactor room. The results of the chemical analysis were obtained at a fixed solution temperature of 25 °C. The uranium concentration was measured by Davies and Gray's method. The uncertainty of the uranium concentration was determined to be 0.7 gU/l. The measurement of free nitric acid concentration was as follows: Initially, the uranium was precipitated by adding (NH<sub>4</sub>)<sub>2</sub>SO<sub>4</sub> and H<sub>2</sub>O<sub>2</sub> to a sample solution. After that, the total acidity was determined by



titration with sodium hydroxide. The free nitric acid concentration was estimated by subtracting the radical of uranyl nitrate from the total acidity. The uncertainty of free nitric acid concentration was determined to be 0.015 mol/l. The solution density was measured by employing a digital density meter. The accuracy of this meter was  $\pm 0.0001 \text{ g/cm}^3$ . The uncertainty including the error of the sampling process was estimated to be  $\pm 0.0006 \text{ g/cm}^3$ .

The temperature of the fuel solution was measured during an operation by the thermocouple inserted in the guide tube within the core tank.

Three elements, Fe, Cr, and Ni, were considered as the main impurities contained in the fuel solution; their concentrations were measured by chemical analysis. The measured concentrations of Fe, Cr and Ni were, respectively, lower than 252 mg/l, 67 mg/l, and 45 mg/l; no analysis of other impurities was made.

The main body of the core tank (the side wall, the lower plate, and the upper plate) and the frame plate of reflector container were made of stainless steel S.S.304L (or SUS304L) and S.S.304(or SUS304), respectively. The measured chemical compositions of those are given in Table 7. The density of stainless steel is  $7.93 \text{ g/cm}^3$  according to the Japanese Industrial Standard (JIS). Other structural material (legs of core tank, tube for thermocouple, guide tube of safety rod, base plate, walls of water-reflector pool tank, fuel feed/drain line, and sheath of  $\text{B}_4\text{C}$  pellets) were also made of stainless steel S.S.304. The containers of the neutron detectors were made of aluminum. The structural materials for fixing the detectors were also made of aluminum.

Table 7. Measured chemical composition of stainless steel (Unit : wt.%).

| Element | Main Body<br>of Core Tank | Frame Plate of<br>Reflector Container |
|---------|---------------------------|---------------------------------------|
| C       | 0.018                     | 0.052                                 |
| Si      | 0.42                      | 0.39                                  |
| Mn      | 1.14                      | 1.16                                  |
| P       | 0.033                     | 0.032                                 |
| S       | 0.007                     | 0.011                                 |
| Ni      | 10.52                     | 8.22                                  |
| Cr      | 18.21                     | 18.29                                 |
| Fe      | 69.652                    | 71.845                                |

The cover plates of the reflector containers were made of aluminum. The measured chemical composition of the aluminum cover plates is given in Table 8. The density of aluminum is  $2.69 \text{ g/cm}^3$ , according to “the Science Table (Japan National Astronomical Observatory)”.

Table 8. Chemical Composition of Aluminum Alloy (Unit : wt.%).

| Al    | Si   | Fe   | Cu   |
|-------|------|------|------|
| 99.20 | 0.14 | 0.59 | 0.07 |

Concrete was used as the reflector material. To determine the chemical composition, the analyses were performed for cylindrical specimens representative of all the reflectors. The averaged bulk density was estimated by measuring the dimensions and the weights for each specimen, and the uncertainty of measurement was  $0.02 \text{ g/cm}^3$ . No significant change of water content in the concrete composition over time was observed. The free-water ratio and the bound-water ratio were estimated by the drying process and the baking process. The measured chemical composition of concrete is given in Table 9. The amounts of other compounds were determined by the chemical analyses. Details of determining the concrete composition are described in Appendix B.

Table 9. Chemical Composition of Concrete.

| Chemical Compound          | ( $\text{g/cm}^3$ )               |
|----------------------------|-----------------------------------|
| free $\text{H}_2\text{O}$  | $0.1145 \pm 0.0028$               |
| bound $\text{H}_2\text{O}$ | $0.1028 \pm 0.0026$               |
| $\text{SiO}_2$             | $1.4716 \pm 0.0281$               |
| $\text{Al}_2\text{O}_3$    | $0.1315 \pm 0.0093$               |
| $\text{Fe}_2\text{O}_3$    | $0.0369 \pm 0.0028$               |
| $\text{CaO}$               | $0.3663 \pm 0.0187$               |
| $\text{MgO}$               | $0.0131 \pm 0.0009$               |
| $\text{SO}_3$              | $0.0145 \pm 0.0012$               |
| $\text{Na}_2\text{O}$      | $0.0542 \pm 0.0081$               |
| $\text{K}_2\text{O}$       | $0.0150 \pm 0.0005$               |
| $\text{Cl}^-$              | $5.3\text{E-}5 \pm 2.3\text{E-}5$ |
| Total                      | $2.321 \pm 0.019$                 |

As indicated in Table 9, total  $\text{H}_2\text{O}$  is  $0.2173 \pm 0.0038 \text{ g/cm}^3$ . The uncertainty is determined by adding uncertainties of free and bound  $\text{H}_2\text{O}$  quadratically, and is about 2%.

#### 1.4 Supplemental Experimental Measurements

As mentioned in Section 1.2, the critical height was determined by reactivity measurement, employing a digital reactivity meter. The differential reactivity worth with respect to solution height was also estimated from this measurement. In a series of experiments employing various reflectors,

the reactivity effects of reflector materials were evaluated by integrating the differential reactivity worth between the critical heights of the objective reflected condition and the reference condition. The main results of these measurements are described in Reference 1.

The neutron flux distribution in the reflector was measured by a gold-wire activation method. The Cd-covered and the uncovered gold wires were positioned in the measuring holes, which penetrated the reflector horizontally and vertically with 5-mm diameter. After high power operation, the gold wires were removed from the measuring holes. The 0.412 MeV photoelectric peak of  $^{198}\text{Au}$  was measured with a 3-inch-thick well-type NaI(Tl) scintillation counter.

For a typical core configuration, the kinetic parameter  $\beta/\lambda$  was also measured by the pulsed neutron method and/or frequency noise analysis. At the present time, the  $\beta/\lambda$  measurement for the slab core tank is written in the unpublished internal report, while the measurement for the 60-cm-diameter core tank is written in the published report.<sup>a</sup>

---

<sup>a</sup> K.Tonoike et al., Proc. ICNC 99, 1215 Versailles, France(1999).

## 2.0 EVALUATION OF EXPERIMENTAL DATA

### 2.1 General Notes

Six critical configurations were collected from the logbook and other unpublished internal documents. The effects on  $k_{\text{eff}}$  of uncertainties in measured data were estimated by sensitivity studies. The sensitivity studies were performed with a two-dimensional transport code, TWOTRAN, and a 16-energy-group cross section set collapsed from the 107-energy-group SRAC public library based on the evaluated nuclear data library, JENDL-3.2. The  $k_{\text{eff}}$ 's were calculated with a convergence criteria of  $1 \times 10^{-5}$ .

For the sensitivity studies, a density formula for uranyl nitrate solution developed at JAERI was used. This formula gives the density of uranyl nitrate solution as a function of uranium concentration, free nitric acid concentration, and solution temperature. The details of this formula are described in Appendix C. This formula was not used to determine the benchmark solution densities. The measured densities at 25°C were used for the benchmark model.

Horizontal XY calculations (X: north-south; Y: east-west) with 6.9-cm extrapolation length in the Z (vertical) direction were performed for the horizontal-dimension sensitivity studies. The XZ calculations with 8.9-cm extrapolation length in the Y direction were done for the vertical-dimension sensitivity studies.

### 2.2 Fuel Solution Uncertainties

As mentioned in Section 1.3, the uncertainties of uranium enrichment, uranium concentration, free nitric acid concentration, and solution density were determined to be 0.013 wt.%, 0.7 gU/l, 0.015 mol/l, and  $0.0006 \text{ g/cm}^3$ , respectively. The solution height was measured with a contact-type level gauge, of which the accuracy was 0.2 mm. The solution temperature was measured with a thermocouple. The temperature change during the operation was estimated to be within 0.3 °C, including accuracy of the device. The concentration of the main impurities Fe, Cr, and Ni were less than 252 mg/l, 67 mg/l, and 45 mg/l, respectively. The effects on  $k_{\text{eff}}$  of uncertainties pertaining to the fuel solution are given in Table 10.

Table 10. Effects on  $k_{\text{eff}}$  of Uncertainties Pertaining to the Fuel Solution. ( $\Delta k_{\text{eff}}$ , %).

| Parameter                    | Variation                      | Run No.     |             |             |             |             |             |
|------------------------------|--------------------------------|-------------|-------------|-------------|-------------|-------------|-------------|
|                              |                                | 133         | 142         | 143         | 144         | 145         | 146         |
| U enrichment                 | $\pm 0.013$ wt. %              | $\pm 0.047$ | $\pm 0.046$ | $\pm 0.046$ | $\pm 0.046$ | $\pm 0.046$ | $\pm 0.047$ |
| U concentration              | $\pm 0.7$ gU/l                 | $\pm 0.059$ | $\pm 0.058$ | $\pm 0.058$ | $\pm 0.058$ | $\pm 0.057$ | $\pm 0.057$ |
| H <sup>+</sup> concentration | $\pm 0.015$ mol/l              | -/+0.022    | -/+0.022    | -/+0.023    | -/+0.022    | -/+0.022    | -/+0.022    |
| Solution density             | $\pm 0.0006$ g/cm <sup>3</sup> | $\pm 0.010$ | $\pm 0.010$ | $\pm 0.010$ | $\pm 0.010$ | $\pm 0.010$ | $\pm 0.010$ |
| Solution height              | $\pm 0.2$ mm                   | $\pm 0.003$ | $\pm 0.002$ | $\pm 0.002$ | $\pm 0.003$ | $\pm 0.003$ | $\pm 0.003$ |
| Temperature                  | $\pm 0.3$ °C                   | -/+0.008    | -/+0.010    | -/+0.010    | -/+0.010    | -/+0.010    | -/+0.011    |
| Impurity (Fe)                | +252 mg/l                      | -0.008      | -0.008      | -0.008      | -0.008      | -0.008      | -0.007      |
| Impurity (Cr)                | +67 mg/l                       | -0.003      | -0.003      | -0.003      | -0.003      | -0.003      | -0.003      |
| Impurity (Ni)                | +45 mg/l                       | -0.002      | -0.002      | -0.002      | -0.002      | -0.002      | -0.002      |
| Total                        |                                | $\pm 0.080$ | $\pm 0.079$ | $\pm 0.079$ | $\pm 0.079$ | $\pm 0.078$ | $\pm 0.079$ |

There are two uncertainties on the temperature:

- (1) The change of temperature during the experiment (0.3°C).
- (2) The fact that atom densities are known at 25°C and the experiments are conducted at other temperatures, a maximum difference of 0.3°C (25-24.7).

The temperature uncertainty has two effects.

- (1) The change in solution density, which is calculated with the density formula;
- (2) The change in uranium concentration C(U).

The following relationships hold for volume, density, and concentration:

$$\begin{aligned} \text{Volume} \times \text{Density} &= \text{Constant}, \\ \text{Volume} \times \text{Concentration} &= \text{Constant}. \end{aligned}$$

Therefore, the following relationships are derived:

$$\Delta V/V = -\Delta \rho/\rho = -\Delta C(U)/C(U).$$

$\Delta C$  may be calculated, since  $\Delta \rho$  is calculated with the density formula. All these effects are included in the  $\Delta k_{\text{eff}}$ 's for temperature in Table 10.

In the sensitivity studies of the impurities, each impurity was added without changing the other constituents of the fuel solution.

### 2.3 Core Tank Uncertainties

The inner thickness of the tank was estimated using the tank outer thickness and double the side-wall thickness. In the same way, the inner width of the tank was estimated using the tank outer width and double the side-wall thickness. The inner height of the tank was estimated using the tank outer height and the upper and lower plate thicknesses.

As to the effects on  $k_{eff}$  of uncertainties pertaining to the core tank, the effects caused by the dimensional uncertainties were evaluated: core thickness, core width, thicknesses of side wall and lower plate. As shown in Table 1, the uncertainties of those were 0.05 cm, 0.05 cm, 0.01 cm, and 0.01 cm, respectively. The effect caused by the stainless steel density was also evaluated. The uncertainty of the density is assumed to be in the least significant digit, 0.01 g/cm<sup>3</sup>. The effects on  $k_{eff}$  of uncertainties pertaining to the core tank were calculated using these uncertainties as variations, and the results are given in Table 11. The calculated effect on  $k_{eff}$  was divided by the square root of the number of measurements (Table 1.b) to obtain the standard deviation of the mean.

Table 11. Effects on  $k_{eff}$  of Uncertainties Pertaining to the Core Tank ( $\Delta k_{eff}$ , %).

| Parameter                              | Variation                 | Run No.     |             |             |             |             |             |
|--|---------------------------|-------------|-------------|-------------|-------------|-------------|-------------|
|  |                           | 133         | 142         | 143         | 144         | 145         | 146         |
| Solution thickness                     | $\pm 0.05\text{cm}$       | $\pm 0.042$ | $\pm 0.046$ | $\pm 0.044$ | $\pm 0.042$ | $\pm 0.041$ | $\pm 0.041$ |
| Solution width                         | $\pm 0.05\text{cm}$       | $\pm 0.006$ | $\pm 0.006$ | $\pm 0.006$ | $\pm 0.006$ | $\pm 0.006$ | $\pm 0.006$ |
| Side-wall thickness (X) <sup>(a)</sup> | $\pm 0.01\text{cm}$       | $\pm 0.003$ | $\pm 0.007$ | $\pm 0.005$ | $\pm 0.004$ | $\pm 0.003$ | $\pm 0.003$ |
| Side-wall thickness (Y) <sup>(b)</sup> | $\pm 0.01\text{cm}$       | $\pm 0.001$ | $\pm 0.001$ | $\pm 0.001$ | $\pm 0.001$ | $\pm 0.001$ | $\pm 0.001$ |
| Lower-plate thickness                  | $\pm 0.01\text{cm}$       | $<0.001$    | $<0.001$    | $<0.001$    | $<0.001$    | $<0.001$    | $\pm 0.001$ |
| Stainless steel density                | $\pm 0.01 \text{ g/cm}^3$ | $\pm 0.002$ | $\pm 0.003$ | $\pm 0.002$ | $\pm 0.002$ | $\pm 0.002$ | $\pm 0.002$ |
| Total                                  |                           | $\pm 0.043$ | $\pm 0.047$ | $\pm 0.045$ | $\pm 0.043$ | $\pm 0.042$ | $\pm 0.042$ |

(a) X: north-south direction

(b) Y: east-west direction

### 2.4 Reflector Uncertainties

As shown in Table 2, the uncertainties of inner wall thickness, concrete thickness, outer wall thickness, and inner gap width were 0.01 cm, less than 0.1 cm, 0.01 cm, and less than 0.1 cm, respectively. As shown in Table 3, the uncertainties of active concrete width was 0.1 cm. And as shown in Table 4, the uncertainties of active concrete height and the lower plate thickness were 0.1 cm and 0.01 cm, respectively. By setting the reflector on the reflector support, the lower ends of the concrete and the active fuel region were adjusted to the same vertical levels. The accuracy of this adjustment were estimated to be 0.1 cm (vertical position of reflector). The uncertainty of the concrete density was estimated to be 0.02 g/cm<sup>3</sup>. The effects on  $k_{eff}$  of uncertainties pertaining to the reflectors are given in Table 12.

Table 12. Effects on  $k_{\text{eff}}$  of Uncertainties Pertaining to Reflectors ( $\Delta k_{\text{eff}}$ , %).

| Parameter             | Variation                    | Run No.     |             |             |             |             |             |
|-----------------------|------------------------------|-------------|-------------|-------------|-------------|-------------|-------------|
|                       |                              | 133         | 142         | 143         | 144         | 145         | 146         |
| Inner gap width       | $\pm 0.10$ cm                | -/+0.025    | -/+0.013    | -/+0.018    | -/+0.024    | -/+0.027    | -/+0.026    |
| Inner wall thickness  | $\pm 0.01$ cm                | $\pm 0.001$ | $\pm 0.003$ | $\pm 0.002$ | $\pm 0.001$ | $\pm 0.001$ | $\pm 0.001$ |
| Concrete thickness    | $\pm 0.10$ cm                | $\pm 0.001$ | $\pm 0.034$ | $\pm 0.019$ | $\pm 0.005$ | $\pm 0.001$ | $\pm 0.001$ |
| Outer wall thickness  | $\pm 0.01$ cm                | <0.001      | $\pm 0.002$ | $\pm 0.001$ | <0.001      | <0.001      | <0.001      |
| Concrete width        | $\pm 0.1$ cm                 | <0.001      | <0.001      | <0.001      | <0.001      | <0.001      | <0.001      |
| Concrete height       | $\pm 0.1$ cm                 | <0.001      | <0.001      | <0.001      | <0.001      | <0.001      | <0.001      |
| Lower plate thickness | $\pm 0.01$ cm                | <0.001      | <0.001      | <0.001      | <0.001      | <0.001      | <0.001      |
| Vertical position     | $\pm 0.1$ cm                 | <0.001      | <0.001      | <0.001      | <0.001      | <0.001      | <0.001      |
| Concrete density      | $\pm 0.02$ g/cm <sup>3</sup> | $\pm 0.005$ | $\pm 0.007$ | $\pm 0.009$ | $\pm 0.007$ | $\pm 0.003$ | $\pm 0.003$ |
| Total                 |                              | $\pm 0.026$ | $\pm 0.037$ | $\pm 0.028$ | $\pm 0.026$ | $\pm 0.027$ | $\pm 0.026$ |

## 2.5 Concrete Composition Uncertainties

As shown in Table 9, the concrete consisted of ten kinds of chemical compounds. The relative uncertainties of each compound were estimated to be less than the following values:

|                                |       |
|--------------------------------|-------|
| H <sub>2</sub> O               | 2.0%; |
| SiO <sub>2</sub>               | 2.0%; |
| Al <sub>2</sub> O <sub>3</sub> | 8.0%; |
| Fe <sub>2</sub> O <sub>3</sub> | 8.0%; |
| CaO                            | 6.0%; |
| MgO                            | 8.0%; |
| SO <sub>3</sub>                | 10%;  |
| Na <sub>2</sub> O              | 20%;  |
| K <sub>2</sub> O               | 5.0%; |
| and Cl <sup>-</sup>            | 50%.  |

The effects on  $k_{\text{eff}}$  of uncertainties pertaining to the concrete composition are given in Table 13.

Table 13. Effects on  $k_{\text{eff}}$  of Uncertainties Pertaining to Concrete Composition ( $\Delta k_{\text{eff}}$ , %).

| Chemical Compound              | Variation (%) | Run No.  |          |          |          |          |          |
|--------------------------------|---------------|----------|----------|----------|----------|----------|----------|
|                                |               | 133      | 142      | 143      | 144      | 145      | 146      |
| H <sub>2</sub> O               | ±2.0%         | -/+0.003 | -/+0.003 | -/+0.003 | -/+0.003 | -/+0.003 | -/+0.003 |
| SiO <sub>2</sub>               | ±2.0%         | ±0.010   | ±0.010   | ±0.010   | ±0.010   | ±0.010   | ±0.010   |
| Al <sub>2</sub> O <sub>3</sub> | ±8.0%         | ±0.005   | ±0.004   | ±0.005   | ±0.005   | ±0.004   | ±0.004   |
| Fe <sub>2</sub> O <sub>3</sub> | ±8.0%         | ±0.001   | ±0.001   | ±0.001   | ±0.001   | ±0.001   | ±0.001   |
| CaO                            | ±6.0%         | ±0.008   | ±0.006   | ±0.008   | ±0.008   | ±0.007   | ±0.007   |
| MgO                            | ±8.0%         | ±0.001   | ±0.001   | ±0.001   | ±0.001   | <0.001   | <0.001   |
| SO <sub>3</sub>                | ±10%          | ±0.001   | ±0.001   | ±0.001   | ±0.001   | ±0.001   | ±0.001   |
| Na <sub>2</sub> O              | ±20%          | ±0.007   | ±0.006   | ±0.008   | ±0.008   | ±0.006   | ±0.006   |
| K <sub>2</sub> O               | ±5.0%         | <0.001   | <0.001   | <0.001   | <0.001   | <0.001   | <0.001   |
| Cl <sup>-</sup>                | ±50%          | <0.001   | <0.001   | <0.001   | <0.001   | <0.001   | <0.001   |
| Total                          |               | ±0.016   | ±0.014   | ±0.016   | ±0.016   | ±0.015   | ±0.015   |

## 2.6 Reactivity Effect of Reflector

The reflector effects of concrete were estimated by TWOTRAN calculations with a convergence criteria of  $1 \times 10^{-5}$ . The definition of the reflector effect is as follows:

$$\rho (\% \Delta k / k) = \left( \frac{1}{k_{\text{eff}}^{(\text{unref})}} - \frac{1}{k_{\text{eff}}^{(\text{ref})}} \right) \times 100,$$

where

$k_{\text{eff}}^{(\text{ref})}$  is  $k_{\text{eff}}$  of the system with a reflector,

$k_{\text{eff}}^{(\text{unref})}$  is  $k_{\text{eff}}$  of the system without a reflector.

The calculated  $k_{\text{eff}}$ 's and the estimated effects are given in Table 14.

Table 14. Evaluated Results of Reflector Effects.

| Run No. | Reflector | Concrete Thickness (cm) | Calculated $k_{\text{eff}}$     |                                   | Reflector Effect (% $\Delta k/k$ ) |
|---------|-----------|-------------------------|---------------------------------|-----------------------------------|------------------------------------|
|         |           |                         | $k_{\text{eff}}^{(\text{ref})}$ | $k_{\text{eff}}^{(\text{unref})}$ |                                    |
| 133     | C150      | 15.00                   | 1.00371                         | 0.97562                           | 2.87                               |
| 142     | C25       | 2.53                    | 1.00587                         | 0.98861                           | 1.74                               |
| 143     | C50       | 5.01                    | 1.00545                         | 0.98261                           | 2.31                               |
| 144     | C100      | 10.07                   | 1.00452                         | 0.97727                           | 2.78                               |
| 145     | C200      | 20.01                   | 1.00358                         | 0.97476                           | 2.95                               |
| 146     | C300      | 30.08                   | 1.00335                         | 0.97464                           | 2.94                               |



## 2.7 Conclusions

The calculated effects of material and geometrical uncertainties are summarized in Table 15 .

Table 15. Summary of Effects on  $k_{\text{eff}}$  for Materials and Geometrical Uncertainties ( $\Delta k_{\text{eff}}$ , %).

| Parameter                         | Run No.     |             |             |             |             |             |
|-----------------------------------|-------------|-------------|-------------|-------------|-------------|-------------|
|                                   | 133         | 142         | 143         | 144         | 145         | 146         |
| Fuel Solution                     | $\pm 0.080$ | $\pm 0.079$ | $\pm 0.079$ | $\pm 0.079$ | $\pm 0.078$ | $\pm 0.079$ |
| Core Tank Dimension and Density   | $\pm 0.043$ | $\pm 0.047$ | $\pm 0.045$ | $\pm 0.043$ | $\pm 0.042$ | $\pm 0.042$ |
| Reflector Dimension and Density   | $\pm 0.026$ | $\pm 0.037$ | $\pm 0.028$ | $\pm 0.026$ | $\pm 0.027$ | $\pm 0.026$ |
| Concrete Composition of Reflector | $\pm 0.016$ | $\pm 0.014$ | $\pm 0.016$ | $\pm 0.016$ | $\pm 0.015$ | $\pm 0.015$ |
| Total                             | $\pm 0.096$ | $\pm 0.100$ | $\pm 0.096$ | $\pm 0.095$ | $\pm 0.094$ | $\pm 0.094$ |

Because the experimental conditions are obviously known and the uncertainties of those have been sufficiently quantified, the six critical configurations included in this evaluation are acceptable benchmark experiments.

### 3.0 BENCHMARK SPECIFICATIONS

#### 3.1 Description of Model

The model consists of the fuel solution, the core tank, the concrete reflectors, and the reflector containers. The following structure and devices are not included in the benchmark model, for simplification:

- (1) Tube for the thermocouple within the core tank.
- (2) Contact-type level gauge. This is above the surface of the fuel solution.
- (3) Four legs supporting the core tank.
- (4) Fuel feed/drain line containing fuel solution. The outer diameter of the tube is 27.2 mm, and its thickness is 3.4 mm.
- (5) Guide tube for the neutron source. This tube lies horizontally below the core tank.
- (6) Base plate supporting four legs. The upper surface of this plate is 14 cm below the bottom of the core tank. The thickness of this plate is 30 mm.
- (7) Beams supporting the base plate. These beams lie on the bottom of the pool tank. The height of these beams is 16 cm.
- (8) Four legs of the reflector support which stand on the bottom of the pool tank (south side) or the base plate (north side). The height of these legs on the south and north sides are 32 cm and 13 cm, respectively.
- (9) Holes penetrating the reflector horizontally and vertically. These holes were prepared to set up neutron detectors or gold wire. The diameter of these holes is 16 mm for neutron detectors, or 5 mm for gold wire.
- (10) Six neutron detectors for reactor operation; two  $^{10}\text{B}$ -lined proportional counters, and four gamma-ray compensated ionization chambers. These were covered with polyethylene to improve the neutron efficiency, and were located beside the reflectors.
- (11) Nine neutron detectors and pulsed neutron source (for Run No. 144.) for the experimental measurements; five  $^3\text{He}$  proportional counters, one  $^{10}\text{B}$ -lined proportional counter and three gamma-ray compensated ionization chambers. The arrangement of neutron detectors for Run No.145 was shown in Figure 5.
- (12) Structures and devices on the top of the core tank; guide tubes of the safety rods, device of the level gauge, safety rods, and so on.
- (13) Side walls and bottom plate of the pool tank. The thickness of the side walls and the bottom plate are 10 mm and 15 mm, respectively. The side wall is at least 39 cm away from the outer surface of the reflector. The bottom plate is 33 cm below the core tank.
- (14) Hood and concrete walls of the reactor room.
- (15) Other structure outside the core tank.
- (16) Holes for gold wires and detectors in the reflector.

To estimate the model simplification effect for each core configuration, a detailed model that includes the structures (1)-(16) was constructed. The model simplification effect is defined as the difference of  $k_{\text{eff}}$ 's between the benchmark model and the detailed model. The calculations of  $k_{\text{eff}}$  were carried out by MCNP4B with JENDL-3.2 ( $10^7$  neutron histories). The estimated results of the model simplification effects are given in Table 16.

Table 16. Estimated Results of Model Simplification Effect.

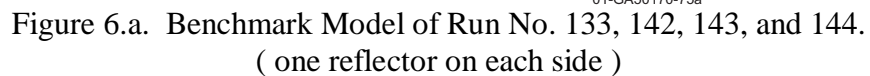
| Run No. | Reflector | Calculated $k_{\text{eff}}$ ( $\pm 1\sigma$ ) |                     | Model Simplification Effect, $\Delta k_{\text{eff}}$ (%) |
|---------|-----------|---|---------------------|--|
|         |           | Benchmark Model                               | Detailed Model      |  |
| 133     | C150      | 1.0069 $\pm$ 0.0002                           | 1.0077 $\pm$ 0.0002 | -0.08 $\pm$ 0.03   |
| 142     | C25       | 1.0075 $\pm$ 0.0002                           | 1.0079 $\pm$ 0.0002 | -0.04 $\pm$ 0.03   |
| 143     | C50       | 1.0080 $\pm$ 0.0002                           | 1.0083 $\pm$ 0.0002 | -0.03 $\pm$ 0.03   |
| 144     | C100      | 1.0075 $\pm$ 0.0002                           | 1.0078 $\pm$ 0.0002 | -0.03 $\pm$ 0.03   |
| 145     | C200      | 1.0071 $\pm$ 0.0002                           | 1.0080 $\pm$ 0.0002 | -0.09 $\pm$ 0.03   |
| 146     | C300      | 1.0075 $\pm$ 0.0002                           | 1.0080 $\pm$ 0.0002 | -0.05 $\pm$ 0.03   |

Because a reflector acts as a neutron isolator of the core tank and the outer objects, it is expected that the model simplification effect decreases as the thickness of concrete increases. As shown in Table 16, however, it was not observed that the model simplification effect depends on the thickness of concrete. Although such a trend in the model simplification effect is not clear in Table 16, values are negative as expected, since most simplifications decrease reflection. It was determined that the model simplification effects should be considered as biases, and the combined standard deviations ( $1\sigma$ ) of the Monte Carlo calculations should be included as the uncertainties.

In the benchmark model, impurities such as Fe, Cr, and Ni are omitted. The reactivity effects of these impurities were obtained in Section 2.2. Because the reactivity effects were estimated with the maximum concentrations during the experiments and the estimated effects were very small, they are not included as biases in the benchmark-model  $k_{\text{eff}}$ 's. But they are included as uncertainties in the benchmark-model  $k_{\text{eff}}$ 's.

### 3.2 Dimensions

The benchmark model with one reflector piece on each of the two larger sides of the core tank is shown in Figure 6.a. The model for Run 145, with a combination of two reflectors on each of the two larger sides, is given in Figure 6.b. And the model for Run 146, with a combination of three reflectors on each of the two larger sides, is given in Figure 6.c. The dimensions of the benchmark model are given in the figure, except the solution height and some horizontal dimensions of the reflector, which are given in Table 17.



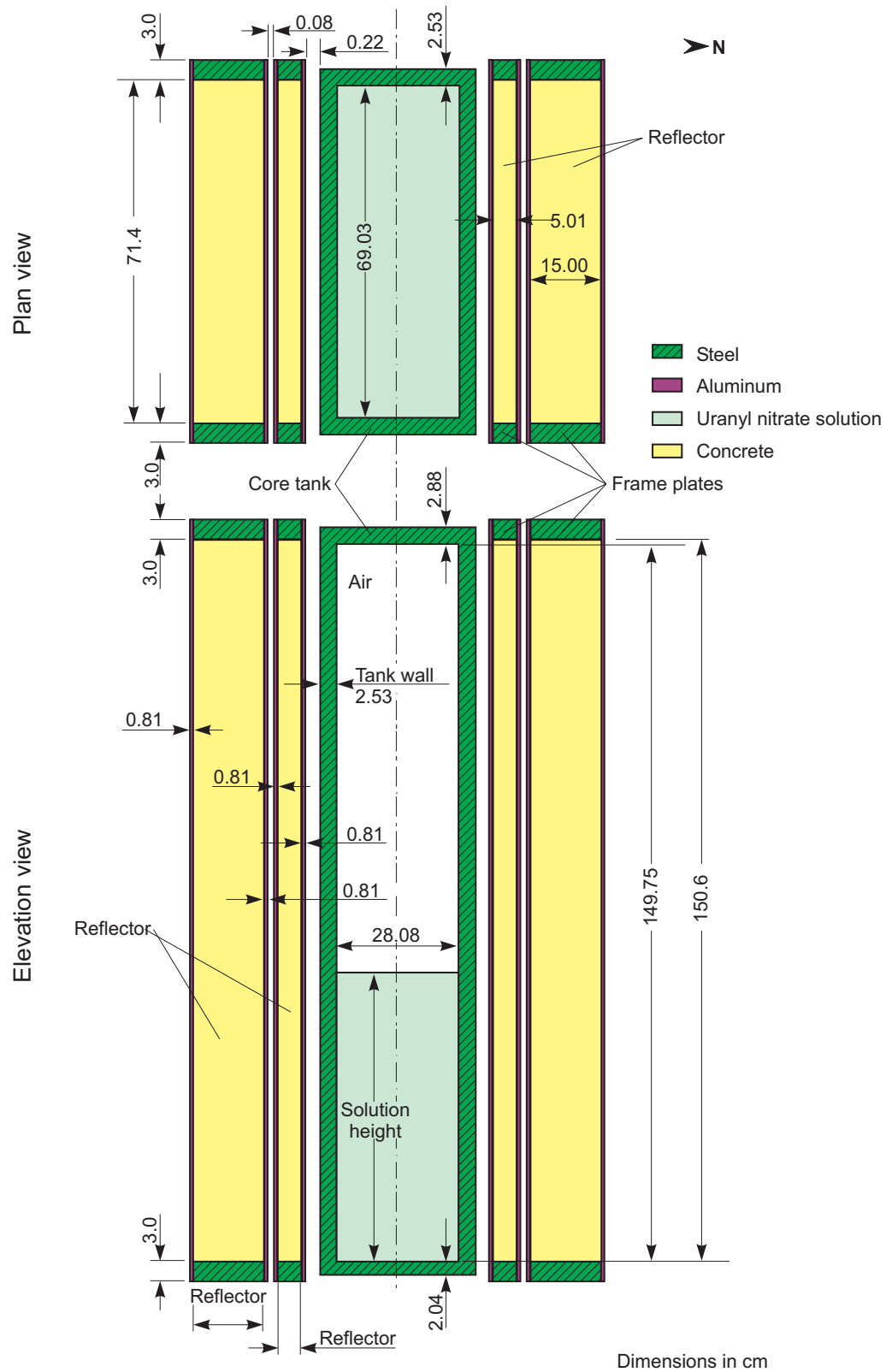


Figure 6.b. Benchmark Model of Run No. 145.  
( combination of two sizes of reflectors on each side )

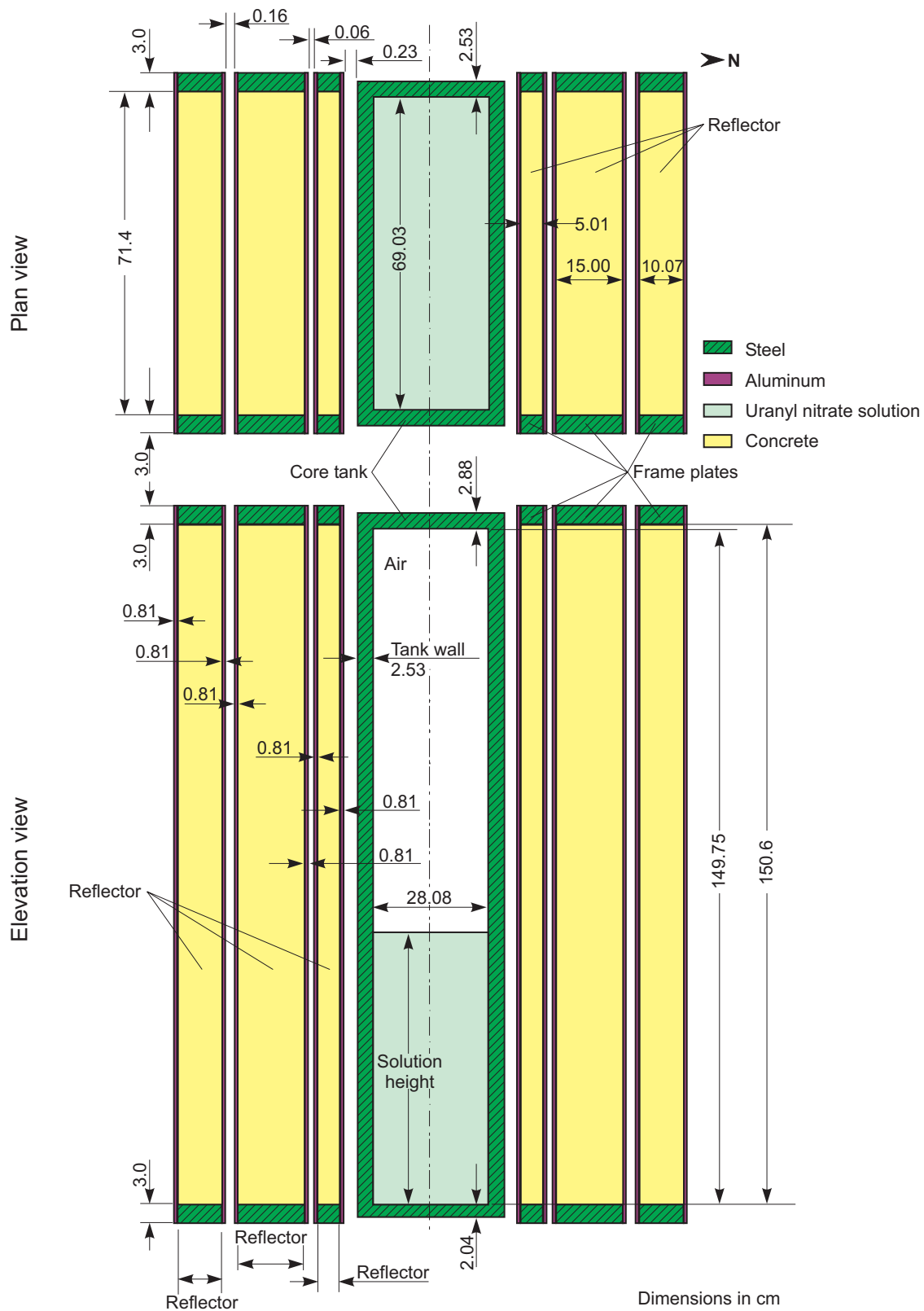


Figure 6.c. Benchmark Model of Run No. 146.  
( combination of three sizes of reflectors on each side )

Table 17. Solution Height and Horizontal Dimensions of Reflector (Unit: cm).

| Run No.                      | Solution Height | Reflector | Horizontal Dimensions of Reflector |            |          |            |
|------------------------------|-----------------|-----------|------------------------------------|------------|----------|------------|
|                              |                 |           | Inner Gap                          | Inner Wall | Concrete | Outer Wall |
| 133                          | 67.91           | C150      | 0.23                               | 0.81       | 15.00    | 0.81       |
| 142                          | 80.57           | C25       | 0.27                               | 0.81       | 2.53     | 0.81       |
| 143                          | 73.18           | C50       | 0.21                               | 0.81       | 5.01     | 0.81       |
| 144                          | 67.95           | C100      | 0.22                               | 0.81       | 10.07    | 0.81       |
| 145 <sup>(a)</sup><br>(C200) | 65.56           | C50       | 0.22                               | 0.81       | 5.01     | 0.81       |
|                              |                 | C150      | 0.08                               | 0.81       | 15.00    | 0.81       |
| 146 <sup>(a)</sup><br>(C300) | 65.00           | C50       | 0.23                               | 0.81       | 5.01     | 0.81       |
|                              |                 | C150      | 0.06                               | 0.81       | 15.00    | 0.81       |
|                              |                 | C100      | 0.16                               | 0.81       | 10.07    | 0.81       |

(a) The reflectors and gaps are listed in order, from the core tank outward.

The core is uranyl nitrate solution in a rectangular stainless steel tank. The tank's inner dimensions are 28.08 cm x 69.03 cm x 149.75 cm high. The four side walls are 2.53 cm thick. The tank bottom is 2.04 cm thick, and the top is 2.88 cm thick. The tank is centered horizontally between the reflectors.

The reflector width is 71.4 cm. And the reflector height is 150.6 cm. The bottom surface of the concrete is level with the bottom of the solution. The thickness of the frame plate is 3.0 cm.

The critical solution heights and the horizontal dimensions of reflectors for each case are summarized in Table 17.

### 3.3 Material Data

The uranium concentration, the free nitric acid concentration, and the solution density at 25°C are known for each core configuration. The atom densities of the fuel solution are given in Table 18. Their derivation is described in Appendix F.

Table 18. Atom Densities of Fuel Solution at 25°C (Unit: atoms/barn-cm).

| Run No. | <sup>234</sup> U | <sup>235</sup> U | <sup>236</sup> U | <sup>238</sup> U | H          | N          | O          |
|---------|------------------|------------------|------------------|------------------|------------|------------|------------|
| 133     | 6.3422E-07       | 7.8702E-05       | 7.8604E-08       | 7.0101E-04       | 5.9135E-02 | 2.0426E-03 | 3.7015E-02 |
| 142     | 6.4266E-07       | 7.9749E-05       | 7.9650E-08       | 7.1034E-04       | 5.8763E-02 | 2.1567E-03 | 3.7146E-02 |
| 143     | 6.4369E-07       | 7.9877E-05       | 7.9777E-08       | 7.1147E-04       | 5.8762E-02 | 2.1593E-03 | 3.7155E-02 |
| 144     | 6.4472E-07       | 8.0005E-05       | 7.9905E-08       | 7.1261E-04       | 5.8746E-02 | 2.1618E-03 | 3.7158E-02 |
| 145     | 6.4595E-07       | 8.0158E-05       | 8.0058E-08       | 7.1398E-04       | 5.8747E-02 | 2.1648E-03 | 3.7170E-02 |
| 146     | 6.4760E-07       | 8.0362E-05       | 8.0262E-08       | 7.1580E-04       | 5.8732E-02 | 2.1689E-03 | 3.7179E-02 |

The density of the stainless steel S.S.304L is 7.93 g/cm<sup>3</sup>. The atom densities of the stainless steel used for the core tank and the frame plates of the reflector containers are given in Table 19.

Table 19. Atom Densities of Stainless Steel (Unit: atoms/barn-cm).

|     | C         | Si        | Mn        | P         | S         | Ni        | Cr        | Fe        |
|-----|-----------|-----------|-----------|-----------|-----------|-----------|-----------|-----------|
| (a) | 7.1567E-5 | 7.1415E-4 | 9.9095E-4 | 5.0879E-5 | 1.0424E-5 | 8.5600E-3 | 1.6725E-2 | 5.9560E-2 |
| (b) | 2.0675E-4 | 6.6314E-4 | 1.0083E-3 | 4.9337E-5 | 1.6380E-5 | 6.6885E-3 | 1.6798E-2 | 6.1435E-2 |

(a) Main body of core tank

(b) Frame plates of reflector container.

The density of aluminum is 2.69 g/cm<sup>3</sup>. The aluminum is used for the cover plates (inner and outer walls) of the reflector containers. The aluminum atom densities are listed in Table 20.

Table 20. Atom Densities of Aluminum Alloy (Unit: atoms/barn-cm).

| Al         | Si         | Fe         | Cu         |
|------------|------------|------------|------------|
| 5.9559E-02 | 8.0751E-05 | 1.7114E-04 | 1.7845E-05 |

The density of concrete is 2.321 g/cm<sup>3</sup>. The chemical composition of the concrete is known in g/cm<sup>3</sup>. The atomic number densities of the concrete are given in Table 21.



Table 21. Atom Density of Concrete.

| Element    | (atoms/barn-cm) |
|------------|-----------------|
| H          | 1.4528E-02      |
| O in water | 7.2639E-03      |
| O in mix   | 3.7326E-02      |
| Na         | 1.0533E-03      |
| Mg         | 1.9573E-04      |
| Al         | 1.5533E-03      |
| Si         | 1.4749E-02      |
| S          | 1.0906E-04      |
| Cl         | 9.0027E-07      |
| K          | 1.9179E-04      |
| Ca         | 3.9337E-03      |
| Fe         | 2.7830E-04      |

It is assumed that the void region above the surface of the fuel solution is occupied by air of density  $0.001184 \text{ g/cm}^3$ . The air is composed of 76.64 wt.% nitrogen and 23.36 wt.% oxygen<sup>a</sup>. The atom density (atoms/barn-cm) of the air is as follows:

3.9014E-05 for nitrogen,  
and 1.0410E-05 for oxygen

### 3.4 Temperature Data

The solution temperature for each core configuration varies from 24.7°C to 25.2°C. However, the solution temperature adopted in the benchmark models is fixed at 25°C because the chemical analyses were performed at this temperature. The effects of the temperature differences were estimated by TWOTRAN calculations with a convergence criteria of  $1 \times 10^{-5}$ . To obtain the atom densities at each temperature, the density formula was used (Appendix C). The calculation was performed considering the change in water density and uranium concentration based on the density formulation, as discussed in Section 2.2. The  $k_{\text{eff}}$ 's at the experimental temperature and at the adopted temperature were calculated. The cross section modification due to the differences of temperature were included in the TWOTRAN calculations. The estimated results of the temperature effects are given in Table 22.

<sup>a</sup> B. TAMAMUSHI et al., Rikagaku Jiten (Science Encyclopedia), Iwanami Shoten (1975) (in Japanese). Other elements were neglected. The wt.% of N and O were adjusted such that the ratio of these were conserved.

Table 22. Evaluated Results of Temperature Effects.

| Run No. | Reflector | Experimental Temperature (°C) | $k_{\text{eff}}$ at 25.0 (°C) | $k_{\text{eff}}$ at Experimental Temperature | Temperature Effect $\Delta k_{\text{eff}}$ (%) |
|---------|-----------|-------------------------------|-------------------------------|--|--|
| 133     | C150      | 24.8                          | 1.00456                       | 1.00461                                      | -0.005   |
| 142     | C25       | 24.9                          | 1.00686                       | 1.00689                                      | -0.003   |
| 143     | C50       | 24.7                          | 1.00649                       | 1.00659                                      | -0.010   |
| 144     | C100      | 25.0                          | 1.00545                       | 1.00545                                      | 0.0  |
| 145     | C200      | 25.2                          | 1.00541                       | 1.00534                                      | +0.007   |
| 146     | C300      | 25.2                          | 1.00418                       | 1.00411                                      | +0.007   |

Each temperature effect is regarded as a bias in the benchmark-model  $k_{\text{eff}}$ .

### 3.5 Experimental and Benchmark-Model $k_{\text{eff}}$

The experimental  $k_{\text{eff}}$ 's are unity. The following sources should be considered as possible biases in the benchmark models:

- (1) model simplification effect – omitting the structures and devices around the core configuration, for simplification,
- (2) impurity effect – excluding the impurities (Fe, Cr, and Ni) from the fuel solution, and
- (3) temperature effect – difference between the experimental temperature and the adopted temperature (25 °C).

Both the model simplification effect and the temperature effect are considered to be biases in the benchmark models. They were estimated in Sections 3.1 and 3.4.

As discussed in Section 3.1, the combined standard deviations ( $1\sigma$ ) of the Monte Carlo calculations of simplifications were also included in the uncertainties. Also, as discussed in Section 3.1, the impurity effects are not included in the biases, but are included in the uncertainties (those pertaining to the fuel solution). In Section 2.0, the uncertainties are estimated as having the following origins:

- (1) fuel solution,
- (2) core tank, and
- (3) reflectors.

The uncertainties of the  $k_{\text{eff}}$ 's included in the benchmark model are obtained by the square root of the sum of individual uncertainties' squares, and correspond to one standard deviation. Consequently, the benchmark-model  $k_{\text{eff}}$ 's are:

LEU-SOL-THERM-018

Run 133 (C150):  $0.9992 \pm 0.0010$ ,  
Run 142 (C25) :  $0.9996 \pm 0.0010$ ,  
Run 143 (C50) :  $0.9996 \pm 0.0010$ ,  
Run 144 (C100):  $0.9997 \pm 0.0010$ ,  
Run 145 (C200):  $0.9992 \pm 0.0010$ , and  
Run 146 (C300):  $0.9996 \pm 0.0010$ .



## 4.0 RESULTS OF SAMPLE CALCULATIONS

The results of the sample calculations using MCNP 4B with the JENDL-3.2 library are given in Table 23.a. These high values are known to be caused by the library's capture cross section of  $^{235}\text{U}$  in the resonance energy range which is smaller than that of the other libraries.

In addition, the CRISTAL code system of IPSN (APOLLO-2 cell code with the CEA93 172-group library based on JEF2.2 evaluation, and MORET-4 Monte Carlo code with  $\sigma=0.03\%$ ) were used for sample calculations. The results are given in Table 23.b. The results of KENO V.a with ENDF/B-IV and V libraries and MCNP4C calculations with ENDF/B-V and VI libraries are given in Table 23.c.

Table 23.a. Sample Calculation Results (Japan).

| Case No. | Code (Cross Section Set) →<br>Run No. (Reflector) ↓ | MCNP<br>(Continuous Energy JENDL-3.2) |
|----------|---|---------------------------------------|
| 1        | 133 (C150)  | $1.0069 \pm 0.0002$                   |
| 2        | 142 (C25)   | $1.0075 \pm 0.0002$                   |
| 3        | 143 (C50)   | $1.0080 \pm 0.0002$                   |
| 4        | 144 (C100)  | $1.0075 \pm 0.0002$                   |
| 5        | 145 (C200)  | $1.0071 \pm 0.0002$                   |
| 6        | 146 (C300)  | $1.0075 \pm 0.0002$                   |

Table 23.b. Sample Calculation Results (France). <sup>(a)</sup>

| Case No. | Code (Cross Section Set) →<br>Run No. (Reflector) ↓ | APOLLO-2 / MORET-4<br>(CEA93 Library-172-Group) |
|----------|---|---|
| 1        | 133 (C150)  | $1.0047 \pm 0.0003$                             |
| 2        | 142 (C25)   | $1.0050 \pm 0.0003$                             |
| 3        | 143 (C50)   | $1.0052 \pm 0.0003$                             |
| 4        | 144 (C100)  | $1.0046 \pm 0.0003$                             |
| 5        | 145 (C200)  | $1.0047 \pm 0.0003$                             |
| 6        | 146 (C300)  | $1.0052 \pm 0.0003$                             |

(a) Results provided by IPSN/DPEA/SEC.

Table 23.c. Sample Calculation Results (United States). <sup>(a)</sup>

| Case No. | Code (Cross Section Set)→<br>Run No. ↓ | KENO                    |                        |                         | MCNP <sup>(b)</sup> |                     |
|----------|--|-------------------------|------------------------|-------------------------|---------------------|---------------------|
|          |  | 27-Group<br>(ENDF/B-IV) | 44-Group<br>(ENDF/B-V) | 238-Group<br>(ENDF/B-V) | ENDF/B-V<br>(.50c)  | ENDF/B-VI<br>(.60c) |
| 1        | 133 (C150)                             | 1.0017 ± 0.0002         | 1.0042 ± 0.0003        | 1.0033 ± 0.0002         | 1.0039 ± 0.0002     | 0.9997 ± 0.0002     |
| 2        | 142 (C25)                              | 1.0019 ± 0.0003         | 1.0043 ± 0.0002        | 1.0039 ± 0.0003         | 1.0043 ± 0.0002     | 1.0002 ± 0.0002     |
| 3        | 143 (C50)                              | 1.0020 ± 0.0003         | 1.0045 ± 0.0003        | 1.0040 ± 0.0003         | 1.0040 ± 0.0002     | 1.0002 ± 0.0002     |
| 4        | 144 (C100)                             | 1.0021 ± 0.0003         | 1.0040 ± 0.0002        | 1.0041 ± 0.0002         | 1.0043 ± 0.0002     | 1.0008 ± 0.0002     |
| 5        | 145 (C200)                             | 1.0016 ± 0.0003         | 1.0035 ± 0.0003        | 1.0037 ± 0.0003         | 1.0043 ± 0.0002     | 0.9999 ± 0.0002     |
| 6        | 146 (C300)                             | 1.0014 ± 0.0003         | 1.0039 ± 0.0002        | 1.0037 ± 0.0003         | 1.0035 ± 0.0002     | 1.0000 ± 0.0002     |

(a) Results provided by Virginia Dean.

(b) Input listings provided by the authors; for ENDF/B-VI calculations, <sup>235</sup>U and <sup>238</sup>U cross sections were Release 4 (.49c).

## 5.0 REFERENCES

1. T. Kikuchi, Y. Miyoshi, Y. Yamane, K. Tonoike, H. Sono, H. Hirose and S. Onodera, "Reflector Effects of Structural Material for Cylindrical and Slab Cores Containing 10% Enriched Uranyl Nitrate Solution," *JAERI-Conf 99-004* (1999).
2. S. Onodera, H. Sono, H. Hirose, Y. Takatsuki, M. Nagasawa, K. Murakami, T. Takahashi, K. Sakuraba, M. Miyauchi, T. Kikuchi, Y. Miyoshi and A. Ohno, "Annual Report of STACY Operation in F.Y. 1997 - 280 mm Thickness Slab Core -- 10% Enriched Uranyl Nitrate Solution - ," (in Japanese) *JAERI-Tech 98-023*(1998).

## **APPENDIX A: TYPICAL INPUT LISTINGS**

### **A.1 MCNP Input Listing**

Japanese MCNP 4B with the continuous-energy cross sections based on the JENDL-3.2 library was run with 2,000 active generations of 5,000 neutrons each (10 million neutron histories), after skipping 50 generations (100,000 neutron histories).

United States MCNP4C calculations used the same inputs files except that cross sections were changed to .50c (sulphur to 16032.50c) for ENDF/B-V and were changed to .60c for ENDF/B-VI.4 (except  $^{235}\text{U}$  and  $^{238}\text{U}$  which were .49c), and 80 generations were run before the 2,000 active generations.

LEU-SOL-THERM-018

MCNP4B Benchmark-Model Input Listing for Run No.145, Table 23.a and Table 16.

STACY 280t Core tank critical analysis.

```
c R145(C200) ;Hc=65.56cm
c
c cell card
c
1 1 9.88764316E-02 1 -2 3 -4 5 -7 imp:n=1 u=1
2 4 4.94240000E-05 1 -2 3 -4 7 -6 imp:n=1 u=1
3 2 8.66829700E-02 #1 #2 imp:n=1 u=1
4 0 11 -12 13 -14 15 -16 imp:n=1 u=2 fill=1
c
11 3 8.11829800E-02 27 -28 32 -33 25 -26 imp:n=1 u=2
12 6 8.68654070E-02 21 -22 32 -33 23 -24 #(27 -28 25 -26) imp:n=1 u=2
13 5 5.98285201E-02 21 -22 31 -34 23 -24 #(32 -33) imp:n=1 u=2
c
14 3 8.11829800E-02 27 -28 37 -36 25 -26 imp:n=1 u=2
15 6 8.68654070E-02 21 -22 37 -36 23 -24 #(27 -28 25 -26) imp:n=1 u=2
16 5 5.98285201E-02 21 -22 38 -35 23 -24 #(37 -36) imp:n=1 u=2
c
17 3 8.11829800E-02 27 -28 40 -41 25 -26 imp:n=1 u=2
18 6 8.68654070E-02 21 -22 40 -41 23 -24 #(27 -28 25 -26) imp:n=1 u=2
19 5 5.98285201E-02 21 -22 39 -42 23 -24 #(40 -41) imp:n=1 u=2
c
20 3 8.11829800E-02 27 -28 45 -44 25 -26 imp:n=1 u=2
21 6 8.68654070E-02 21 -22 45 -44 23 -24 #(27 -28 25 -26) imp:n=1 u=2
22 5 5.98285201E-02 21 -22 46 -43 23 -24 #(45 -44) imp:n=1 u=2
23 4 4.94240000E-05 #4 #(21 -22 31 -34 23 -24) #(21 -22 38 -35 23 -24)
      #(21 -22 39 -42 23 -24) #(21 -22 46 -43 23 -24)
      imp:n=1 u=2
100 0 81 -82 83 -84 85 -86 imp:n=1 fill=2
101 0 #100 imp:n=0
c
c surface cards (origin x=0.0 y=0.0 z=0.0)
c fuel
1 px -34.515
2 px 34.515
3 py -14.04
4 py 14.04
5 pz 0.0
6 pz 149.75
c Critical level
7 pz 65.56
c sus304
c
11 px -37.045
12 px 37.045
13 py -16.57
14 py 16.57
15 pz -2.04
16 pz 152.63
c c150 reflector
c
21 px -38.7
22 px 38.7
23 pz -3.0
24 pz 153.6
25 pz 0.0
26 pz 150.6
27 px -35.7
28 px 35.7
31 py 16.79
32 py 17.60
33 py 22.61
34 py 23.42
35 py -16.79
36 py -17.60
```



LEU-SOL-THERM-018

MCNP4B Benchmark-Model Input Listing for Run No.145, Table 23.a and Table 16 (cont'd).

```

37 py -22.61
38 py -23.42
39 py 23.50
40 py 24.31
41 py 39.31
42 py 40.12
43 py -23.50
44 py -24.31
45 py -39.31
46 py -40.12
c pool
c
81 px -111.0
82 px 291.0
83 py -100.0
84 py 100.0
85 pz -34.5
86 pz 172.63

c
c data cards
c
mode n          $ transport neutrons only
c
c material cards
c
c R145(C200);U=313.8/A=0.955/D=1.4500
c atomic density = 9.88764316E-02
m1 1001.37c 5.8747E-02
    7014.37c 2.1648E-03
    8016.37c 3.7170E-02
    92234.37c 6.4595E-07
    92235.37c 8.0158E-05
    92236.37c 8.0058E-08
    92238.37c 7.1398E-04
mt1 lwtr.01t $ 300k
c
c sus304L(tank) 7.93g/cm3
c atomic density 8.668297E-2
m2 6012.37c 7.1567E-05 $ C
    14000.37c 7.1415E-04 $ Si
    25055.37c 9.9095E-04 $ Mn
    15031.37c 5.0879E-05 $ P
    16000.37c 1.0424E-05 $ S
    28000.37c 8.5600E-03 $ Ni
    24000.37c 1.6725E-02 $ Cr
    26000.37c 5.9560E-02 $ Fe
c
c concrete (STACY-280T) T-ave.
c atomic density 8.11829800E-02
m3 1001.37c 1.4528e-02
    8016.37c 4.4590E-02
    11023.37c 1.0533E-03
    12000.37c 1.9573E-04
    13027.37c 1.5533E-03
    14000.37c 1.4749E-02
    16000.37c 1.0906E-04
    17000.37c 9.0027E-07
    19000.37c 1.9179E-04
    20000.37c 3.9337E-03
    26000.37c 2.7830E-04
mt3 lwtr.01t $ 300k
c
c air (0.001184 g/cm3)
c atomic density 4.9424E-05
m4 7014.37c 3.9014E-05
    8016.37c 1.0410E-05

```

LEU-SOL-THERM-018

MCNP4B Benchmark-Model Input Listing for Run No.145, Table 23.a and Table 16 (cont'd).

```
c
c aluminum 2.69 g/cm3
c atomic density 5.98285201E-02
m5 13027.37c 5.9559E-02 $ Al
    14000.37c 8.0751E-05 $ Si
    26000.37c 1.7114E-04 $ Fe
    29000.37c 1.7845E-05 $ Cu
c
c sus304L(futa) 7.93g/cm3
c atomic density 8.68654070e-02
m6 6012.37c 2.0675E-04 $ C
    14000.37c 6.6314E-04 $ Si
    25055.37c 1.0083E-03 $ Mn
    15031.37c 4.9337E-05 $ P
    16000.37c 1.6380E-05 $ S
    28000.37c 6.6885E-03 $ Ni
    24000.37c 1.6798E-02 $ Cr
    26000.37c 6.1435E-02 $ Fe
c
c criticality cards
c
kcode 5000 1.0 50 2050
sdef cel=d1 x=d2 y=d3 z=d4 erg=d5
c
si1 1 100:4:1
sp1 1
c *** x-coordinate
si2 h -34.5 34.5
sp2 0 1
c *** y-coordinate
si3 h -14.0 14.0
sp3 0 1
c *** z-coordinate
si4 h 0.0 65.56
sp4 0 1
c
sp5 -3
c
prdmp j -100 1 3
c
print -175
c ctme 10
```

LEU-SOL-THERM-018

MCNP4C ENDF/B-VI.4 Benchmark-Model Input Listing for Run No.146, Table 23.c.

STACY 280t Core tank critical analysis.

```
c R146(C300) ;Hc=65.0 cm
c
c cellcard
c
1 1 9.88761485E-02 1 -2 3 -4 5 -7 imp:n=1 u=1
2 4 4.94240000E-05 1 -2 3 -4 7 -6 imp:n=1 u=1
3 2 8.66829700E-02 #1 #2 imp:n=1 u=1
4 0 11 -12 13 -14 15 -16 imp:n=1 u=2 fill=1
c
11 3 8.11829800E-02 27 -28 32 -33 25 -26 imp:n=1 u=2
12 6 8.68654070E-02 21 -22 32 -33 23 -24 #(27 -28 25 -26) imp:n=1 u=2
13 5 5.98285201E-02 21 -22 31 -34 23 -24 #(32 -33) imp:n=1 u=2
c
14 3 8.11829800E-02 27 -28 37 -36 25 -26 imp:n=1 u=2
15 6 8.68654070E-02 21 -22 37 -36 23 -24 #(27 -28 25 -26) imp:n=1 u=2
16 5 5.98285201E-02 21 -22 38 -35 23 -24 #(37 -36) imp:n=1 u=2
c
17 3 8.11829800E-02 27 -28 40 -41 25 -26 imp:n=1 u=2
18 6 8.68654070E-02 21 -22 40 -41 23 -24 #(27 -28 25 -26) imp:n=1 u=2
19 5 5.98285201E-02 21 -22 39 -42 23 -24 #(40 -41) imp:n=1 u=2
c
20 3 8.11829800E-02 27 -28 45 -44 25 -26 imp:n=1 u=2
21 6 8.68654070E-02 21 -22 45 -44 23 -24 #(27 -28 25 -26) imp:n=1 u=2
22 5 5.98285201E-02 21 -22 46 -43 23 -24 #(45 -44) imp:n=1 u=2
c
23 3 8.11829800E-02 27 -28 48 -49 25 -26 imp:n=1 u=2
24 6 8.68654070E-02 21 -22 48 -49 23 -24 #(27 -28 25 -26) imp:n=1 u=2
25 5 5.98285201E-02 21 -22 47 -50 23 -24 #(48 -49) imp:n=1 u=2
c
26 3 8.11829800E-02 27 -28 53 -52 25 -26 imp:n=1 u=2
27 6 8.68654070E-02 21 -22 53 -52 23 -24 #(27 -28 25 -26) imp:n=1 u=2
28 5 5.98285201E-02 21 -22 54 -51 23 -24 #(53 -52) imp:n=1 u=2
29 4 4.94240000E-05 #4 #(21 -22 31 -34 23 -24) #(21 -22 38 -35 23 -24)
      #(21 -22 39 -42 23 -24) #(21 -22 46 -43 23 -24)
      #(21 -22 47 -50 23 -24) #(21 -22 54 -51 23 -24)
      imp:n=1 u=2
100 0 81 -82 83 -84 85 -86 imp:n=1 fill=2
101 0 #100 imp:n=0
c
c surface cards (origin x=0.0 y=0.0 z=0.0)
c fuel
1 px -34.515
2 px 34.515
3 py -14.04
4 py 14.04
5 pz 0.0
6 pz 149.75
c Critical level
7 pz 65.0
c sus304
c
11 px -37.045
12 px 37.045
13 py -16.57
14 py 16.57
15 pz -2.04
16 pz 152.63
c c50+c150+c100 reflector
c
21 px -38.7
22 px 38.7
23 pz -3.0
24 pz 153.6
25 pz 0.0
```

LEU-SOL-THERM-018

MCNP4C ENDF/B-VI.4 Benchmark-Model Input Listing for Run No.146, Table 23.c (cont'd).

```

26 pz 150.6
27 px -35.7
28 px 35.7
31 py 16.80
32 py 17.61
33 py 22.62
34 py 23.43
35 py -16.80
36 py -17.61
37 py -22.62
38 py -23.43
39 py 23.49
40 py 24.30
41 py 39.30
42 py 40.11
43 py -23.49
44 py -24.30
45 py -39.30
46 py -40.11
47 py 40.27
48 py 41.08
49 py 51.15
50 py 51.96
51 py -40.27
52 py -41.08
53 py -51.15
54 py -51.96
c pool
c
81 px -111.0
82 px 291.0
83 py -100.0
84 py 100.0
85 pz -34.5
86 pz 172.5

c
c data cards
c
mode n $ transfort neutrons only
c
c material cards
c
c R146(C300);U=314.6/A=0.955/D=1.4511
c atomic density = 9.88761485E-02
m1 1001.60c 5.8732E-02
    7014.60c 2.1689E-03
    8016.60c 3.7179E-02
    92234.60c 6.4760E-07
    92235.49c 8.0362E-05
    92236.60c 8.0262E-08
    92238.49c 7.1580E-04
mt1 lwtr.01t $ 300k
c
c sus304L(tank) 7.93g/cm3
c atomic density 8.668297E-2
m2 6000.60c 7.1567E-05 $ C
    14000.60c 7.1415E-04 $ Si
    25055.60c 9.9095E-04 $ Mn
    15031.60c 5.0879E-05 $ P
    16032.60c 1.0424E-05 $ S
    28058.60c 5.8439E-03 $ Ni
    28060.60c 2.2342E-03
    28061.60c 9.6728E-05
    28062.60c 3.0730E-04
    28064.60c 7.7896E-05
    26054.60c 3.5140E-03 $ Fe

```

LEU-SOL-THERM-018

MCNP4C ENDF/B-VI.4 Benchmark-Model Input Listing for Run No.146, Table 23.c (cont'd).

```

26056.60c 5.4628E-02
26057.60c 1.2508E-03
26058.60c 1.6677E-04
24050.60c 7.2669E-04 $ Cr
24052.60c 1.4014E-02
24053.60c 1.5889E-03
24054.60c 3.9554E-04
c concrete (STACY-280T) T-ave.
c atomic density 8.11829800E-02
m3 1001.60c 1.4528e-02
8016.60c 4.4590E-02
11023.60c 1.0533E-03
12000.60c 1.9573E-04
13027.60c 1.5533E-03
14000.60c 1.4749E-02
16032.60c 1.0906E-04
17000.60c 9.0027E-07
19000.60c 1.9179E-04
20000.60c 3.9337E-03
26054.60c 1.6420E-05
26056.60c 2.5526E-04
26057.60c 5.8444E-06
26058.60c 7.7925E-07
mt3 lwtr.01t $ 300k
c
c air (0.001184 g/cm3)
c atomic density 4.9424E-05
m4 7014.60c 3.9014E-05
8016.60c 1.0410E-05
c
c alminum 2.69 g/cm3
c atomic density 5.98285201E-02
m5 13027.60c 5.9559E-02 $ Al
14000.60c 8.0751E-05 $ Si
26054.60c 1.0097E-05 $ Fe
26056.60c 1.5697E-04
26057.60c 3.5939E-06
26058.60c 4.7919E-07
29063.60c 1.2343E-05 $ Cu
29065.60c 5.5015E-06
c
c sus304L(futa) 7.93g/cm3
c atomic density 8.68654070e-02
m6 6000.60c 2.0675E-04 $ C
14000.60c 6.6314E-04 $ Si
25055.60c 1.0083E-03 $ Mn
15031.60c 4.9337E-05 $ P
16032.60c 1.6380E-05 $ S
28058.60c 4.5662E-03 $ Ni
28060.60c 1.7457E-03
28061.60c 7.5580E-05
28062.60c 2.4012E-04
28064.60c 6.0865E-05
24050.60c 7.2989E-04 $ Cr
24052.60c 1.4075E-02
24053.60c 1.5958E-03
24054.60c 3.9728E-04
26054.60c 3.6246E-03 $ Fe
26056.60c 5.6348E-02
26057.60c 1.2901E-03
26058.60c 1.7202E-04
c
c criticality cards
c
kcode 5000 1.0 80 2080
sdef cel=d1 x=d2 y=d3 z=d4 erg=d5

```

LEU-SOL-THERM-018

MCNP4C ENDF/B-VI.4 Benchmark-Model Input Listing for Run No.146, Table 23.c (cont'd).

```
c
si1 1 100:4:1
sp1 1
c *** x-coordinate
si2 h -34.5 34.5
sp2 0 1
c *** y-coordinate
si3 h -14.0 14.0
sp3 0 1
c *** z-coordinate
si4 h 0.0 65.0
sp4 0 1
c
sp5 -3
c
prdmp j -100 1 3
c
print -175
c ctme 10
```

## **A.2 CRISTAL: APOLLO-2 / MORET-4 Input Listing**

The calculations of  $k_{\text{eff}}$ 's were run in two steps, using the CRISTAL code system.

- 1) APOLLO-2 is a one-dimensional multigroup cell code. It is used to determine material buckling  $B_m^2$ , infinite multiplication factor ( $k_{\text{inf}}$ ), and homogeneous macroscopic medium cross sections.
- 2) MORET-4 is a three-dimensional multigroup Monte Carlo code. It uses macroscopic cross sections coming from APOLLO-2. It uses P5 anisotropic treatment and 172-group library. Each calculation employed 1,000 neutrons per batch and was run to achieve precision of 0.0010.

The APOLLO-2 used the CEA93 172-group library based on JEF2.2 evaluation. A pre-processor called CIGALES-PREAPOL is used to prepare the APOLLO-2 input data.

Page 47 of 77



LEU-SOL-THERM-018

CRISTAL Input Listing for Run No.133, Table 23.b (cont'd).

```

      &SNNN &TRAC &P0 &DIFF ANISO &TRAN ANISO ;
*
*      -- Creation de la Macrolib pour le milieu MILHOM1 --
*
APOTRIM: &EDIT 1 TSTR.nom_calc.'MAC' ANISO
      &FICH 47 &NOMMIL TSTR.'MILREF'.nom_mil nom_mil ;
=====
* APOLLO PIJ CALCUL 2
=====
*
* core tank stainless steel
TITRE: 'core tank stainless steel' ;
WRITE: TOPT.'RESU' '*core tank stainless steel' ;
*
*      -- Description des milieux --
*****
TSTR TOPT = INITIALISER_CRISTAL 1 TSTR TOPT ;
*core tank stainless steel
nom_calc = 'MILHOM2' ;
TOPT.'STCRI'. 'CALCUL_INITIAL' = nom_calc ;
TOPT.'STCRI'. 'CALCULS_INITIAUX'.nom_calc = TABLE: ;
TSTR.nom_calc = TABLE: ;
*
nom_mil = 'core tank stainless st' ;
TOPT.'STMIL'.nom_mil = TABLE: ;
TOPT.'STMIL'.nom_mil.'FENAT' ' = 5.95600E-02 ;
TOPT.'STMIL'.nom_mil.'CRNAT' ' = 1.67248E-02 ;
TOPT.'STMIL'.nom_mil.'NINAT' ' = 8.55998E-03 ;
TOPT.'STMIL'.nom_mil.'MN55' ' = 9.90953E-04 ;
TOPT.'STMIL'.nom_mil.'SINAT' ' = 7.14148E-04 ;
TOPT.'STMIL'.nom_mil.'CNAT' ' = 7.15673E-05 ;
TOPT.'STMIL'.nom_mil.'P31' ' = 5.08793E-05 ;
TOPT.'STMIL'.nom_mil.'S32' ' = 1.04556E-05 ;
TOPT.'STMIL'.nom_mil.'TEMPERATURE' = 25. ;
*
TRES TSTR TOPT = GENERE_MILIEUX_S 2 TSTR TOPT ;
*
*      -- Creation de la geometrie --
*
TSTR.nom_calc.'GEO' = GEOM: &CYLI &MAIL 1 &EQD 1.
      &MILI TSTR.'MILREF'.nom_mil 1 ;
*
*      -- Creation de la bibliotheque interne --
*
TSTR.'APOLIB' = BIBINT: &EDIT 1 TSTR.'APOLIB'
      TSTR.'IDB' TSTR.nom_calc.'GEO'
      ( TEXTE TOPT.'REPBIB' ) ;
*
TSTR.nom_calc.'MAC' = MACROLIB: &EDIT TOPT.'STIMP'. 'MACROLIB'
      TSTR.'MILREF'.nom_mil
      &TOTA &SELF &ABSO &ENER &FISS &ENER
      &SNNN &TRAC &P0 &DIFF ANISO &TRAN ANISO ;
*
*      -- Creation de la Macrolib pour le milieu MILHOM2 --
*
APOTRIM: &EDIT 1 TSTR.nom_calc.'MAC' ANISO &NOMA
      &FICH 47 &NOMMIL TSTR.'MILREF'.nom_mil nom_mil ;
=====
* APOLLO PIJ CALCUL 3
=====
*
*stacy * run 133 CAS 3
TITRE: 'stacy * run 133' CAS 3 ' ;
WRITE: TOPT.'RESU' 'NITR ANALY C(U)=308.100 C(PU)=0.000 '
' CAS 3 ' ;
*
*      -- Description des milieux --

```

LEU-SOL-THERM-018

CRISTAL Input Listing for Run No.133, Table 23.b (cont'd).

```
*****
TSTR TOPT = INITIALISER_CRISTAL 1 TSTR TOPT          ;
*NITR ANALY C(U)=308.100 C(PU)=0.000 H+=0.80 =0.00
nom_calc = 'MILHOM3'                                ;
TOPT.'STCRI'. 'CALCUL_INITIAL' = nom_calc            ;
TOPT.'STCRI'. 'CALCULS_INITIAUX'. nom_calc = TABLE:  ;
TSTR.nom_calc = TABLE:                              ;
*
nom_mil = 'NITR ANALY C(U)=308,10'                   ;
TOPT.'STMIL'. nom_mil = TABLE:                      ;
TOPT.'STMIL'. nom_mil.'U234'   ' = 6.34217E-07       ;
TOPT.'STMIL'. nom_mil.'U235'   ' = 7.87020E-05       ;
TOPT.'STMIL'. nom_mil.'U236'   ' = 7.86038E-08       ;
TOPT.'STMIL'. nom_mil.'U238'   ' = 7.01008E-04       ;
TOPT.'STMIL'. nom_mil.'H2O'    ' = 2.95676E-02       ;
TOPT.'STMIL'. nom_mil.'O16'    ' = 7.44780E-03       ;
TOPT.'STMIL'. nom_mil.'N14'    ' = 2.04261E-03       ;
TOPT.'STMIL'. nom_mil.'TEMPERATURE' = 25.            ;
*
TRES TSTR TOPT = GENERE_MILIEUX_S 2 TSTR TOPT        ;
*
*      --- Creation de la geometrie ---
*
TSTR.nom_calc.'GEO' = GEOM: &CYLI &MAIL 1 &EQD 1.
                &MILI TSTR.'MILREF'. nom_mil 1      ;
*
*      --- Creation de la bibliotheque interne ---
*
TSTR.'APOLIB' = BIBINT: &EDIT 1 TSTR.'APOLIB'
                TSTR.'IDB' TSTR.nom_calc.'GEO'
                ( TEXTE TOPT.'REPBIB' )              ;
*
*      --- autoprotection ---
*
TSTR.'GEOAU' = TSTR.nom_calc.'GEO'                  ;
*
TRES TSTR TOPT = AUTOPROTECTION_CRI_S 1 TSTR TOPT    ;
*
*      --- Flux a B2 nul ---
*
TOPT.'TYPE_B2' = 'NUL'                              ;
TRES TSTR TOPT = CALFLUX_PIJ_CRI_S 1 TSTR TOPT      ;
*
*      --- Flux a B2 critique ---
*
SI ( TRES.'KINF' GT 1. )                             ;
TOPT.'TYPE_B2' = 'CRITIQUE'                          ;
TRES TSTR TOPT = CALFLUX_PIJ_CRI_S 1 TSTR TOPT      ;
FINSI                                                ;
*
TOPT.'STCRI'. 'CALCULS_INITIAUX'. nom_calc.'B2' = TRES.'B2' ;
TOPT.'STCRI'. 'CALCULS_INITIAUX'. nom_calc.'KINF' = TRES.'KINF' ;
*
*      --- Condensation homogeneisation ---
*
TRES TSTR TOPT = HOMOGES_COND_S 1 TSTR TOPT          ;
*
*      --- Creation de la Macrolib pour le milieu MILHOM3 ---
*
APOTRIM: &EDIT 1 TSTR.nom_calc.'MAC' ANISO &NOMA
        &FICH 47 &NOMMIL TSTR.nom_calc.'MILEQ' nom_mil ;
*=====
* APOLLO PIJ CALCUL 4
*=====
*
* reflector frame stainless steel
```

LEU-SOL-THERM-018

CRISTAL Input Listing for Run No.133, Table 23.b (cont'd).

```
TITRE: 'reflector frame stainless steel' ;
WRITE: TOPT.'RESU' '*reflector frame stainless steel' ;
*
*      -- Description des milieux --
*****
TSTR TOPT = INITIALISER_CRISTAL 1 TSTR TOPT ;
*reflector frame stainless steel
nom_calc = 'MILHOM4' ;
TOPT.'STCRI'. 'CALCUL_INITIAL' = nom_calc ;
TOPT.'STCRI'. 'CALCULS_INITIAUX'. nom_calc = TABLE: ;
TSTR.nom_calc = TABLE: ;
*
nom_mil = 'reflector frame stainl' ;
TOPT.'STMIL'. nom_mil = TABLE: ;
TOPT.'STMIL'. nom_mil. 'FENAT' = 6.14353E-02 ;
TOPT.'STMIL'. nom_mil. 'CRNAT' = 1.67983E-02 ;
TOPT.'STMIL'. nom_mil. 'NINAT' = 6.68850E-03 ;
TOPT.'STMIL'. nom_mil. 'MN55' = 1.00834E-03 ;
TOPT.'STMIL'. nom_mil. 'SINAT' = 6.63138E-04 ;
TOPT.'STMIL'. nom_mil. 'CNAT' = 2.06750E-04 ;
TOPT.'STMIL'. nom_mil. 'P31' = 4.93375E-05 ;
TOPT.'STMIL'. nom_mil. 'S32' = 1.64302E-05 ;
TOPT.'STMIL'. nom_mil. 'TEMPERATURE' = 25. ;
*
TRES TSTR TOPT = GENERE_MILIEUX_S 2 TSTR TOPT ;
*
*      -- Creation de la geometrie --
*
TSTR.nom_calc. 'GEO' = GEOM: &CYLI &MAIL 1 &EQD 1.
&MILI TSTR. 'MILREF'. nom_mil 1 ;
*
*      -- Creation de la bibliotheque interne --
*
TSTR. 'APOLIB' = BIBINT: &EDIT 1 TSTR. 'APOLIB'
TSTR. 'IDB' TSTR. nom_calc. 'GEO'
( TEXTE TOPT. 'REPBIB' ) ;
*
TSTR. nom_calc. 'MAC' = MACROLIB: &EDIT TOPT. 'STIMP'. 'MACROLIB'
TSTR. 'MILREF'. nom_mil
&TOTA &SELF &ABSO &ENER &FISS &ENER
&SNNN &TRAC &P0 &DIFF ANISO &TRAN ANISO ;
*
*      -- Creation de la Macrolib pour le milieu MILHOM4 --
*
APOTRIM: &EDIT 1 TSTR. nom_calc. 'MAC' ANISO &NOMA
&FICH 47 &NOMMIL TSTR. 'MILREF'. nom_mil nom_mil ;
*
=====
* APOLLO PIJ CALCUL 5
=====
*
* relector Aluminium alloy
TITRE: 'relector Aluminium alloy' ;
WRITE: TOPT.'RESU' '*relector Aluminium alloy' ;
*
*      -- Description des milieux --
*****
TSTR TOPT = INITIALISER_CRISTAL 1 TSTR TOPT ;
*relector Aluminium alloy
nom_calc = 'MILHOM5' ;
TOPT.'STCRI'. 'CALCUL_INITIAL' = nom_calc ;
TOPT.'STCRI'. 'CALCULS_INITIAUX'. nom_calc = TABLE: ;
TSTR.nom_calc = TABLE: ;
*
nom_mil = 'relector Aluminium all' ;
TOPT.'STMIL'. nom_mil = TABLE: ;
TOPT.'STMIL'. nom_mil. 'AL27' = 5.95588E-02 ;
TOPT.'STMIL'. nom_mil. 'SINAT' = 8.07507E-05 ;
```

LEU-SOL-THERM-018

CRISTAL Input Listing for Run No.133, Table 23.b (cont'd).

```

TOPT.'STMIL'.nom_mil.'FENAT'  =  1.71140E-04      ;
TOPT.'STMIL'.nom_mil.'CUNAT'  =  1.78447E-05      ;
TOPT.'STMIL'.nom_mil.'TEMPERATURE' =  25.          ;
*
TRES TSTR TOPT = GENERE_MILIEUX_S 2 TSTR TOPT      ;
*
*      -- Creation de la geometrie --
*
TSTR.nom_calc.'GEO' = GEOM: &CYLI &MAIL 1 &EQD 1.
      &MILI TSTR.'MILREF'.nom_mil 1      ;
*
*      -- Creation de la bibliotheque interne --
*
TSTR.'APOLIB' = BIBINT: &EDIT 1 TSTR.'APOLIB'
      TSTR.'IDB' TSTR.nom_calc.'GEO'
      ( TEXTE TOPT.'REPBIB' )      ;
*
TSTR.nom_calc.'MAC' = MACROLIB: &EDIT TOPT.'STIMP'.MACROLIB'
      TSTR.'MILREF'.nom_mil
      &TOTA &SELF &ABSO &ENER &FISS &ENER
      &SNNN &TRAC &P0 &DIFF ANISO &TRAN ANISO      ;
*
*      -- Creation de la Macrolib pour le milieu MILHOM5 --
*
APOTRIM: &EDIT 1 TSTR.nom_calc.'MAC' ANISO &NOMA
      &FICH 47 &NOMMIL TSTR.'MILREF'.nom_mil nom_mil      ;
*=====
* APOLLO PIJ CALCUL 6
*=====
*
* stacy : concrete reflector
TITRE: ' stacy : concrete reflector      ' ;
WRITE: TOPT.'RESU' '*stacy : concrete reflector      ' ;
*
*      -- Description des milieux --
*****
TSTR TOPT = INITIALISER_CRISTAL 1 TSTR TOPT      ;
*stacy : concrete reflector
nom_calc = 'MILHOM6'      ;
TOPT.'STCRI'.CALCUL_INITIAL' = nom_calc      ;
TOPT.'STCRI'.CALCULS_INITIAUX'.nom_calc = TABLE:      ;
TSTR.nom_calc = TABLE:      ;
*
nom_mil = 'stacy : concrete refle'      ;
TOPT.'STMIL'.nom_mil = TABLE:      ;
TOPT.'STMIL'.nom_mil.'NA23'  =  1.05330E-03      ;
TOPT.'STMIL'.nom_mil.'MGNAT'  =  1.95730E-04      ;
TOPT.'STMIL'.nom_mil.'AL27'  =  1.55330E-03      ;
TOPT.'STMIL'.nom_mil.'SINAT'  =  1.47490E-02      ;
TOPT.'STMIL'.nom_mil.'S32'   =  1.09060E-04      ;
TOPT.'STMIL'.nom_mil.'CLNAT'  =  9.00270E-07      ;
TOPT.'STMIL'.nom_mil.'KNAT'   =  1.91790E-04      ;
TOPT.'STMIL'.nom_mil.'CANAT'  =  3.93370E-03      ;
TOPT.'STMIL'.nom_mil.'FENAT'  =  2.78300E-04      ;
TOPT.'STMIL'.nom_mil.'H2O'    =  7.26390E-03      ;
TOPT.'STMIL'.nom_mil.'O16'    =  3.73260E-02      ;
TOPT.'STMIL'.nom_mil.'TEMPERATURE' =  25.          ;
*
TRES TSTR TOPT = GENERE_MILIEUX_S 2 TSTR TOPT      ;
*
*      -- Creation de la geometrie --
*
TSTR.nom_calc.'GEO' = GEOM: &CYLI &MAIL 1 &EQD 1.
      &MILI TSTR.'MILREF'.nom_mil 1      ;
*
*      -- Creation de la bibliotheque interne --

```

Page 52 of 77

Revision: 0  
Date: September 30, 2001

LEU-SOL-THERM-018

CRISTAL Input Listing for Run No.133, Table 23.b (cont'd).

```
*MN55      1.16
*SINAT      0.39
*CNAT       0.052
*P31        0.032
*S32        0.011
)
OPTION V4 GROUP 172 P5 TEMPER 25 FINOPTION
MORET
GEOM HOMO
CHIMIE
*reflector frame stainless steel
MICRO 1 8  FENAT  CRNAT  NINAT  MN55  SINAT
      CNAT  P31  S32
CONC      6.14353E-02 1.67983E-02 6.68850E-03 1.00834E-03 6.63138E-04
      2.06750E-04 4.93375E-05 1.64302E-05
FINC
SECTION TOUT
FIN
(
  reflector Aluminum alloy
  *reflector Aluminum alloy
  ***** Milieu 1 %-prop MASSIQUES- Dens= 2.69- %volumique 100
  *AL27      99.2
  *SINAT      0.14
  *FENAT      0.59
  *CUNAT      0.07
)
OPTION V4 GROUP 172 P5 TEMPER 25 FINOPTION
MORET
GEOM HOMO
CHIMIE
*reflector Aluminum alloy
MICRO 1 4  AL27  SINAT  FENAT  CUNAT
CONC      5.95588E-02 8.07507E-05 1.71140E-04 1.78447E-05
FINC
SECTION TOUT
FIN
(
  stacy : concrete reflector
  *stacy : concrete reflector
  ***** Milieu 1 CONC. ATOMIQUES- %volumique 100
  *NA23      1.0533E-03
  *MGNAT      1.9573E-04
  *AL27      1.5533E-03
  *SINAT      1.4749E-02
  *S32      1.0906E-04
  *CLNAT      9.0027E-07
  *KNAT      1.9179E-04
  *CANAT      3.9337E-03
  *FENAT      2.7830E-04
  *H2O      7.2639E-03
  *O16      3.7326E-02
)
OPTION V4 GROUP 172 P5 TEMPER 25 FINOPTION
MORET
GEOM HOMO
CHIMIE
*stacy : concrete reflector
MICRO 1 11 NA23  MGNAT  AL27  SINAT  S32
      CLNAT  KNAT  CANAT  FENAT  H2O
      O16
CONC      1.05330E-03 1.95730E-04 1.55330E-03 1.47490E-02 1.09060E-04
      9.00270E-07 1.91790E-04 3.93370E-03 2.78300E-04 7.26390E-03
      3.73260E-02
FINC
SECTION TOUT
FIND
```

LEU-SOL-THERM-018

CRISTAL Input Listing for Run No.133, Table 23.b (cont'd).

```

DEBUT_MORET4
  ICSBEP    LEU-SOL-THERM-018    RUN 133
*
* U(9.97%)O2(NO3)2    C(U)=308.1 g/l H+=0.800  *
*
* CRITICAL HEIGHT 67.91  CONCRETE REFLECTED C150 *
* .....
*
* benchmark Keff = 1.0000 +/- 0.0014      *
*
*****
* precision
  SIGI 0.00033 SIGE 0.00033 MINI 100 PAS 50  NOBIL
* SIGI 0.015 SIGE 0.015  MINI 10 NOBIL
* medium
* 1 *- air
* 2 *- tank wall stainless steel
* 3 *- U(10)O2(NO3)2 solution
* 4 *- reflector frame stainless steel
* 5 *- reflector sheet aluminum alloy
* 6 *- concrete
CHIMIE
  SEALINK 6 APO2    6  1 2 3 4 5 6
FINCHIMIE
*
GEOMETRY
** core tank
* ..... air external volume .....
  TYPE 1 BOITE 100 100 100
  VOLUME 1 0 1 1  0.0 0.0 100
* ..... tank : st.st. SUS 304 L .....
  TYPE 2 BOITE 16.57 37.045 77.335
  VOLUME 2 1 2 2  0.0 0.0 78.295
* ..... air .....
  TYPE 3 BOITE 14.04 34.515 74.875
  VOLUME 3 2 3 1  0.0 0.0 77.875
* ..... fissile solution Hc = 67.91 cm altitude = Hc + 3
  TYPE 4 PLAZ INF 70.91
  VOLUME 4 3 4 3  0.0 0.0 52.0  ETSUP 1 3
** reflectors C150 : AL / ST.ST. / CONCRETE
  TYPE 5 BOITE 8.31 38.7 78.3
  TYPE 6 BOITE 7.5  38.7 78.3
  TYPE 7 BOITE 7.5  35.7 75.3

  VOLUME 5 1 5 5 25.11 0.0 78.3
  VOLUME 6 5 6 4 25.11 0.0 78.3
  VOLUME 7 6 7 6 25.11 0.0 78.3

  VOLUME 15 1 5 5 -25.11 0.0 78.3
  VOLUME 16 15 6 4 -25.11 0.0 78.3
  VOLUME 17 16 7 6 -25.11 0.0 78.3
FINGEOMETRY
* ..... sources .....
  SOURCE NRES POINT 1000 4 0.0 0.0 35.0
  FINSOURCE
* GRAPH Z 100 FGRAPH
SORTIE
MAIL 1 5 21 48 95 135 172
GLOBAL
FSORTIE
FINDATA
FIN_MORET4

```



### **A.3 KENO Input Listing**

KENO V.a with the 238-group ENDF/B-V cross section library from SCALE4.4 was run with 1020 active generations of 9999 neutrons each (10 million neutron histories), after skipping 80 generations (799,920 neutron histories).

LEU-SOL-THERM-018

KENO V.a 238-group ENDF/B-V Benchmark-Model Input Listing for Run No.146, Table 23.c.

```
=C SAS25  PARM=SIZE=4500000
LST18-6, STACY RUN 146, 28-CM SLAB OF U(10)O2(NO3)2 SOLN, 30-CM-THK CONCRETE REFL
238GROUPNDF5 MULTIREGION
' U(9.97)O2(NO3)2 SOLUTION
U-234 1 0 6.4760E-07  END
U-235 1 0 8.0362E-05  END
U-236 1 0 8.0262E-08  END
U-238 1 0 7.1580E-04  END
H 1 0 5.8732E-02  END
N 1 0 2.1689E-03  END
O 1 0 3.7179E-02  END
' SS Tank
C 2 0 7.1567E-05  END
Si 2 0 7.1415E-04  END
Mn 2 0 9.9095E-04  END
P 2 0 5.0879E-05  END
S 2 0 1.0424E-05  END
Ni 2 0 8.5600E-03  END
Cr 2 0 1.6725E-02  END
Fe 2 0 5.9560E-02  END
' SS Frame Plates
C 3 0 2.0675E-04  END
Si 3 0 6.6314E-04  END
Mn 3 0 1.0083E-03  END
P 3 0 4.9337E-05  END
S 3 0 1.6380E-05  END
Ni 3 0 6.6885E-03  END
Cr 3 0 1.6798E-02  END
Fe 3 0 6.1434E-02  END
' Aluminum cover plates of reflector
Al 4 0 5.9559E-02  END
Si 4 0 8.0751E-05  END
Fe 4 0 1.7114E-04  END
Cu 4 0 1.7845E-05  END
' Concrete
H 5 0 1.4528E-02  END
O 5 0 4.45899E-02  END
Na 5 0 1.0533E-03  END
Mg 5 0 1.9573E-04  END
Al 5 0 1.5533E-03  END
Si 5 0 1.4749E-02  END
S 5 0 1.0906E-04  END
Cl 5 0 9.0027E-07  END
K 5 0 1.9179E-04  END
Ca 5 0 3.9337E-03  END
Fe 5 0 2.7830E-04  END
' Air
N 6 0 3.9014E-05  END
O 6 0 1.0410E-05  END
END COMP
BUCKLED SLAB VAC REFL 0.0 69.03 65  END
1 14.04 2 16.57 0 16.80 4 17.61 5 47.61  END ZONE
LST18-6, STACY RUN 146, 28-CM SLAB OF U(10)O2(NO3)2 SOLN, 30-CM-THK CONCRETE REFL
READ PARA TME=200 GEN=1100 NPG=9999 NSK=80 NUB=YES XS1=YES RUN=YES
END PARA
READ GEOM
UNIT 1
COM=* SOLUTION IN TANK, INNER GAP *
CUBOID 1 1 28.08 0.0 69.03 0.0 65.00 0.0
CUBOID 6 1 28.08 0.0 69.03 0.0 149.75 0.0
REPLICATE 2 1 4R2.53 2.88 2.04 1
REPLICATE 0 1 2R0.23 2R1.655 0.97 0.96 1
UNIT 2
COM=* FIRST CONCRETE REFLECTOR *
CUBOID 5 1 5.01 0.0 71.4 0.0 150.6 0.0
CUBOID 3 1 5.01 0.0 74.4 -3.0 153.6 -3.0
```

LEU-SOL-THERM-018

KENO V.a 238-group ENDF/B-V Benchmark-Model Input Listing for Run No.146, Table 23.c (cont'd).

```
REPLICATE 4 1 2R0.81 4R0 1
UNIT 3
COM=* SECOND CONCRETE REFLECTOR *
CUBOID 5 1 15.0 0.0 71.4 0.0 150.6 0.0
CUBOID 3 1 15.0 0.0 74.4 -3.0 153.6 -3.0
REPLICATE 4 1 2R0.81 4R0 1
UNIT 4
COM=* THIRD CONCRETE REFLECTOR *
CUBOID 5 1 10.07 0.0 71.4 0.0 150.6 0.0
CUBOID 3 1 10.07 0.0 74.4 -3.0 153.6 -3.0
REPLICATE 4 1 2R0.81 4R0 1
UNIT 5
COM=* FIRST GAP BETWEEN CONCRETE REFLECTORS *
CUBOID 0 1 0.06 0.0 74.4 -3.0 153.6 -3.0
UNIT 6
COM=* SECOND GAP BETWEEN CONCRETE REFLECTORS *
CUBOID 0 1 0.16 0.0 74.4 -3.0 153.6 -3.0
GLOBAL
UNIT 7
COM=* REFLECTOR, TANK, REFLECTOR *
ARRAY 1 3R0
END GEOM
READ START NST=1 END START
READ ARRAY ARA=1 NUX=11 FILL 4 6 3 5 2 1 2 5 3 6 4 END FILL
END ARRAY
READ PLOT
TTL="HORIZONTAL CROSS SECTION"
LPI=10 XUL=-2.0 YUL=80. ZUL=10 XLR=106.0 YLR=-2.0
ZLR=10 UAX=1 VDN=-1 NAX=1200 NCH='S23*ca' END
TTL="VERTICAL CROSS SECTION"
XUL=-2.0 YUL=30. ZUL=160 XLR=106.0 YLR=30.0
ZLR=-2 UAX=1 WDN=-1 NAX=1200 NCH='S23*ca' END
END PLOT
END DATA
END
```

## APPENDIX B: CONCRETE COMPOSITION

The aim of this appendix is to describe the concrete-composition analysis carried out.

Concrete reflectors were built by pouring the concrete directly into the slab-shaped containers. The reflectors were manufactured in 3 steps:

- mixing together sand and pebbles (mainly  $\text{SiO}_2$ ), cement, and water,
- casting of the mixture in the slab-shaped container,
- covering of concrete until set for preventing evaporation of water.

Samples for analysis were manufactured at the same time. Samples were made by pouring concrete into a vinyl-chloride tube, which had an inner diameter of 10 cm, and a height of 140 cm (almost the same as the active height of the reflector). The manufacture of the reflectors was finished at the end of 1996, a year before the start of the experiments.

The analyses of the chemical compositions were carried out in the autumn of 1997 and at the beginning of 2001. Each sample was divided vertically into three parts: top, middle, and bottom parts. The sampling positions are shown in Table B.1. The analyses were carried out mainly for seven middle parts and one bottom part. No significant change of water content in the concrete composition over time was observed.

Table B.1. Sampling Position of Reflector Material.

| Reflector | Side   |                             |
|-----------|--------|-----------------------------|
|           | north  | south                       |
| C25       | ---    | middle                      |
| C50       | ---    | middle                      |
| C100      | middle | middle                      |
| C150      | middle | middle (2 parts),<br>bottom |

Three specimens - X, Y, and Z specimens - were prepared from each part. Therefore, there were 24 specimens. The sampling methods for each specimen are shown in Figures B.1 and B.2.

The following analyses were performed:

X specimen - Three bulk densities were estimated by measuring the dimensions and weight: in the collected condition, wet condition, and dried condition. The wet and dried conditions mean the condition after soaking in water for 24 hours, or after drying at  $110^\circ\text{C}$  for 7-10 days, respectively.

Y specimen - Two bulk densities were estimated by measuring the dimensions and weight

in the collected and dried conditions. The dried condition means the same as the above definition. The dried Y specimen was crushed to powder, and the chemical analysis was carried out.

Z specimen - Two kinds of bulk densities were estimated by measuring the dimensions and weight: in the collected and dried conditions. Here, the dried condition means the condition after drying at 110°C for 24 days. The content of bound water was measured, using the dried Z specimen. (The method will be described later.)

All 24 specimens had data for the bulk density in the collected and dried conditions. The average of those in the collected condition is  $(2.321 \pm 0.019) \text{ g/cm}^3$ . The ratio of free water to the dried condition is defined as follows:

$$R_{\text{freeH}_2\text{O}} (\%) = \frac{\text{density}_{\text{collected}} - \text{density}_{\text{dried}}}{\text{density}_{\text{dried}}} \times 100 .$$

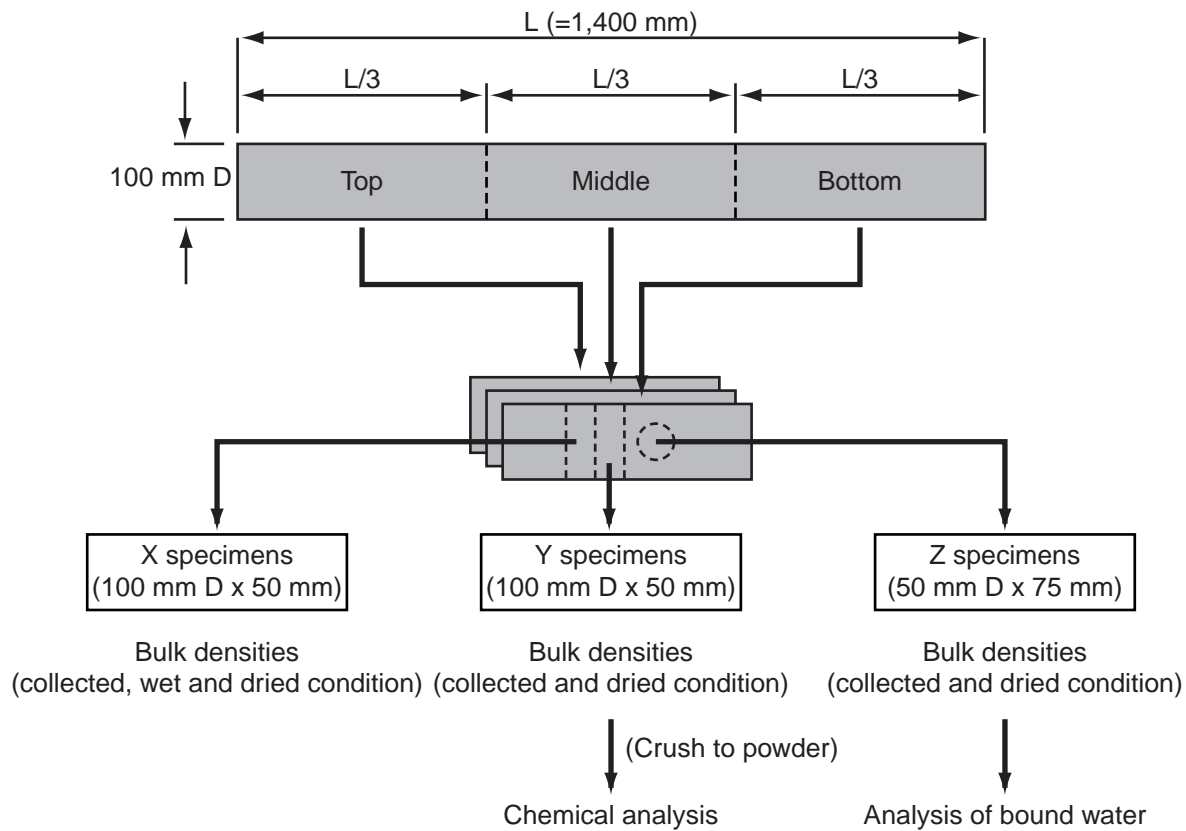
The ratios of free water were estimated for all 24 specimens. The drying processes of X and Y specimens were stopped when mass decreases were no longer observed (7-10 days). From the viewpoint of drying term, the free-water ratio measured for the Z specimen should be larger than those of X and Y specimens, if the composition of concrete were uniform. However, the ratios of free water measured for Z specimens were not always larger than those for X and Y specimens. The final value of the ratio of free water estimated from the average of 24 data is  $(5.19 \pm 0.12)\%$ .

The bulk density in the dried condition was estimated from that in the collected condition and the ratio of free water:

$$\text{density}_{\text{dried}} = \frac{100 \cdot \text{density}_{\text{collected}}}{R_{\text{freeH}_2\text{O}} (\%) + 100} ,$$

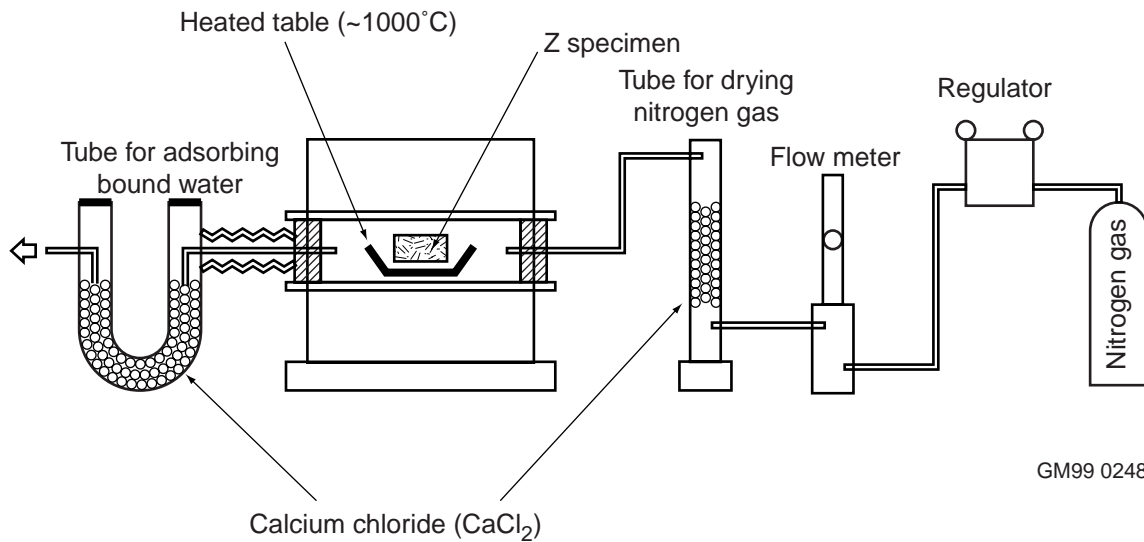
and the estimated value is  $(2.206 \pm 0.018) \text{ g/cm}^3$ .

The content of bound water was measured on eight Z specimens. The schematic view of the equipment is shown in Figure B.2. The specimen was set on the heated table in a nitrogen atmosphere. The temperature around the heated table was above 1000 °C, and the specimen was baked for about 2 hours. The bound water was adsorbed onto calcium chloride ( $\text{CaCl}_2$ ) at the outlet. (Calcium chloride in the inlet adsorbed any water in the nitrogen gas.) The content of bound water was estimated from the mass increase of calcium chloride at the outlet. The averaged ratio of bound water to the dried condition (mass of specimen before heating) is  $(4.66 \pm 0.11)\%$ .



GM99 0247

Figure B.1. Sampling Method of Specimens.



GM99 0248

Figure B.2. Schematic View of the Equipment Used for Analysis of Bound Water.

The chemical analyses were carried out on the concrete powder made from eight dried Y specimens, based on JIS R5202 (Japanese Industrial Standard: Method for chemical analysis of Portland cement). The measured results of the chemical analysis are given in Table B.2, in which the average and the standard deviation for each chemical compound are listed. The bound water is included in the dried Y specimen. However, the sum of wt.% of bound water and the total wt.% of measured chemical compounds is not 100 wt.%. It is thought that this discrepancy was caused by the existence of chemical compounds in various forms ( $\text{Fe}_2\text{O}_3 \rightarrow \text{Fe}_3\text{O}_4$ ,  $\text{CaO} \rightarrow \text{CaCO}_3$ , etc.). The chemical composition without the free and bound water was determined by assuming that the existing ratios were kept. For convenience, the normalized ratios, which total 100 wt.%, are also given in Table B.2.

Table B.2. Result of Chemical Analysis on Concrete Powder (Unit: wt.%).

| Chemical Compound       | Measured            | Normalized <sup>(b)</sup> |
|-------------------------|---------------------|---------------------------|
| $\text{SiO}_2$          | $63.8 \pm 1.1$      | $70.0 \pm 1.2$            |
| $\text{Al}_2\text{O}_3$ | $5.70 \pm 0.40$     | $6.25 \pm 0.44$           |
| $\text{Fe}_2\text{O}_3$ | $1.60 \pm 0.12$     | $1.75 \pm 0.13$           |
| $\text{CaO}$            | $15.88 \pm 0.80$    | $17.43 \pm 0.88$          |
| $\text{MgO}$            | $0.57 \pm 0.04$     | $0.62 \pm 0.04$           |
| $\text{SO}_3$           | $0.63 \pm 0.05$     | $0.69 \pm 0.05$           |
| $\text{Na}_2\text{O}$   | $2.35 \pm 0.35$     | $2.58 \pm 0.38$           |
| $\text{K}_2\text{O}$    | $0.65 \pm 0.02$     | $0.71 \pm 0.02$           |
| $\text{Cl}^-$           | $0.0023 \pm 0.0010$ | $0.0025 \pm 0.0011$       |
| Total                   | $91.1823^{(a)}$     | (100.0325)                |

(a) Extra digit used for normalization is shown.

(b) These values are shown only for information: the measured values and total of those are used for the derivation of each compound's density, in fact.

Each chemical component is given in  $\text{g/cm}^3$  (Table 9). Using the bulk density in the dried condition and the ratio of free water and bound water to the dried condition, the densities of free and bound water are estimated as follows:

$$\begin{aligned}
 \text{density}_{\text{free H}_2\text{O}} &= \text{density}_{\text{dried}} \times R_{\text{free H}_2\text{O}} \\
 &= (2.206 \pm 0.018) \times (0.0519 \pm 0.0012) \\
 &= (0.1145 \pm 0.0028) \text{ g/cm}^3 \\
 \text{density}_{\text{bound H}_2\text{O}} &= \text{density}_{\text{dried}} \times R_{\text{bound H}_2\text{O}} \\
 &= (2.206 \pm 0.018) \times (0.0466 \pm 0.0011) \\
 &= (0.1028 \pm 0.0026) \text{ g/cm}^3
 \end{aligned}$$

The densities of other compounds are estimated using the bulk density in the dried condition, the ratios of all compounds without bound water, and the normalized ratio of each compound to the dried condition. For example, the density of  $\text{SiO}_2$  is estimated as follows:

$$\begin{aligned} \text{density}_{SiO_2} &= \text{density}_{dried} \times (1 - R_{bound\ H_2O}) \times \text{normalized}_{SiO_2} \\ &= (2.206 \pm 0.018) \times (0.9534 \pm 0.0011) \times (63.8 \pm 1.1) / 91.1823 \\ &= (1.4716 \pm 0.0281) \text{ g/cm}^3 \end{aligned}$$

The uncertainties are derived as follows:

$$d = D \times \{(a/A)^2 + (b/B)^2 + (c/C)^2\}^{1/2}$$

where     A and a are value and uncertainty of *density<sub>dried</sub>*,  
              B and b are value and uncertainty of  $(1 - R_{bound\ H_2O})$ ,  
              C and c are value and uncertainty of *normalized<sub>SiO2</sub>*, and  
              D and d are value and uncertainty of *density<sub>SiO2</sub>*.

Values of other compounds are given in Table 9.



**APPENDIX C: DENSITY FORMULA<sup>a</sup>**

The density formula usable for U(VI)-nitrate aqueous solution, Pu(IV)-nitrate aqueous solution and U(VI)-Pu(IV)-nitrate aqueous solution was used for sensitivity calculations in Section 2 and for calculating the bias in the benchmark-model  $k_{\text{eff}}$  due to temperature. The equation is as follows:

$$\begin{aligned}\rho = & 0.99833 + 1.6903 \times 10^{-3} \cdot C_{Pu25} + 1.4276 \times 10^{-3} \cdot C_{U25} \\ & + 3.9956 \times 10^{-2} \cdot C_{HN25} - 8.696 \times 10^{-8} \cdot (C_{Pu25})^2 \\ & - 1.087 \times 10^{-7} \cdot (C_{U25})^2 - 8.513 \times 10^{-4} \cdot (C_{HN25})^2 \\ & - 5.442 \times 10^{-6} \cdot T^2 - 4.4889 \times 10^{-5} \cdot C_{Pu25} \cdot C_{HN25} \\ & - 1.310 \times 10^{-6} \cdot C_{Pu25} \cdot T - 1.564 \times 10^{-5} \cdot C_{U25} \cdot C_{HN25} \\ & - 9.487 \times 10^{-7} \cdot C_{U25} \cdot T - 8.684 \times 10^{-5} \cdot C_{HN25} \cdot T,\end{aligned}$$

where

- $\rho$  : density of solution at T (g/cm<sup>3</sup>),
- $C_{Pu25}$  : concentration of plutonium at 25°C (g/liter),
- $C_{U25}$  : concentration of uranium at 25°C (g/liter),
- $C_{HN25}$  : concentration of free nitric acid at 25°C (mol/liter),
- $T$  : temperature (°C).

The equation is valid under the following conditions:

- $C_{U25} < 530$  g/liter,
- $C_{Pu25} < 480$  g/liter,
- $C_{Pu25} + C_{U25} < 350$  g/liter (valid for mixed fuel solution),
- $C_{HN25} < 7$  mol/liter,
- $10 < T < 60$  °C.

The accuracy of this equation is 0.0032 g/cm<sup>3</sup>.

---

<sup>a</sup> S. Sakurai and S. Tachimori, "Modified density equation for aqueous solutions with plutonium (IV), uranium (IV) and nitric acid," JAERI-M 88-127 (1988) (in Japanese).

## APPENDIX D: HOLES IN REFLECTORS FOR MEASURING DEVICES

Table D.1. Number of Holes and Total Volume.

| item<br>reflecror | reflector<br>dimensions ( cm ) |                  |       | number of holes<br>for gold wire<br>( 0.5 cm dia.) |   |   | number of holes<br>for measurement<br>( 1.6 cm dia. ) |   |   | volume of<br>reflector<br>V(cm <sup>3</sup> ) | volume of<br>holes<br>v(cm <sup>3</sup> ) | volume<br>fraction of<br>holes<br>v/V(%) |
|-------------------|--------------------------------|------------------|-------|--|---|---|---|---|---|---|---|--|
|                   | X <sup>(a)</sup>               | Y <sup>(a)</sup> | Z     | X  | Y | Z | X   | Y | Z |   |   |  |
| C25               | 2.53                           | 71.4             | 150.6 | 6  |   |   | 2   |   |   | 27205   | 13.15                                     | 0.048                                    |
| C50               | 5.01                           | 71.5             | 150.5 | 6  |   |   | 2   |   |   | 53911   | 26.05                                     | 0.048                                    |
| C100              | 10.07                          | 71.4             | 150.6 | 6  | 2 | 2 | 2   |   | 2 | 108281  | 745.14                                    | 0.688                                    |
| C150              | 15.00                          | 71.4             | 150.7 | 6  |   | 2 | 2   | 2 | 4 | 161400  | 1636.29                                   | 1.014                                    |

(a) X is north-south direction, Y is east-west direction

**APPENDIX E: MCNP4B DETAILED-MODEL INPUT LISTING**

The MCNP4B detailed-model input listing for Run No.145, Table 16, is provided below. The continuous-energy cross sections based on the JENDL-3.2 library were used. MCNP4B was run with 2,000 active generations of 5,000 neutrons each (10 million neutron histories), after skipping 50 generations (100,000 neutron histories).

```

file name=run145; STACY ( model 5 )
c FUEL UO2(NO3)2
c Hc = 65.56 cm
c 200T Concrete
c Tank is all considered.
c
c cell card
c
221 2 8.66829700E-02 #(-226 227 -231) -226 1 -230 imp:n=1 u=2
222 2 8.66829700E-02 227 -2 -228 229 imp:n=1 u=2
223 4 4.94240000E-05 227 -2 -229 imp:n=1 u=2
224 4 4.94240000E-05 -229 2 -3 imp:n=1 u=2
225 2 8.66829700E-02 229 -228 2 -3 imp:n=1 u=2
226 1 9.88764316E-02 -500 501 -233 imp:n=1 u=2
1 1 9.88764316E-02 1 -2 11 -12 13 -14 228 #221 imp:n=1 u=2
2 4 4.94240000E-05 228 2 -3 11 -12 13 -14 imp:n=1 u=2
3 2 8.66829700E-02 -4 #(11 -12 13 -14 1 -3) #226
  #(3 -229) #(3 -221) #(3 -222) #(3 -223) imp:n=1 u=2
70 2 8.66829700E-02 #(4 -221 -225) -171 4
  #(330 -331) imp:n=1 u=2
261 19 1.37809E-01 330 -331 imp:n=1 u=2
71 2 8.66829700E-02 #(4 -222 -225) -172 4
  #(330 -332) imp:n=1 u=2
262 19 1.37809E-01 330 -332 imp:n=1 u=2
72 2 8.66829700E-02 #(4 -223 -225) -173 4
  #(330 -333) imp:n=1 u=2
263 19 1.37809E-01 330 -333 imp:n=1 u=2
74 2 8.66829700E-02 4 -176 -175 imp:n=1 u=2
75 2 8.66829700E-02 4 -177 imp:n=1 u=2
76 2 8.66829700E-02 4 -178 imp:n=1 u=2
77 2 8.66829700E-02 4 -179 imp:n=1 u=2
210 2 8.66829700E-02 4 -220 imp:n=1 u=2
170 4 4.94240000E-05 3 -221 -225 imp:n=1 u=2
171 4 4.94240000E-05 3 -222 -225 imp:n=1 u=2
172 4 4.94240000E-05 3 -223 -225 imp:n=1 u=2
174 4 4.94240000E-05 3 -4 -229 imp:n=1 u=2
78 4 4.94240000E-05 #(11 -12 13 -14 1 -3) #3 #70 #71 #72
  #210 #74 #75 #76 #77
  #170 #171 #172 #174 #226
  #261 #262 #263
  imp:n=1 u=2
79 0 5 15 -16 17 -18 imp:n=1 u=3 fill=2
c NS guide pipe
c 250 4 4.94240000E-05 -531 imp:n=1 u=3
c 251 2 8.66829700E-02 531 -532 imp:n=1 u=3
c 252 4 4.94240000E-05 532 -533 imp:n=1 u=3
c 253 2 8.66829700E-02 533 -534 imp:n=1 u=3
c 12 2 8.66829700E-02 41 -42 imp:n=1 u=3
c 163 4 4.94240000E-05 534 -41 imp:n=1 u=3
c
c Foot of tank
4 2 8.66829700E-02 (15 -16 51 -52 -5 43):
  (15 -16 52 -53 -57 43) imp:n=1 u=3
5 2 8.66829700E-02 (15 -16 -54 55 -5 43):
  (15 -16 -55 56 -57 43) imp:n=1 u=3
c
c fuel feed pipe 1
c

```

LEU-SOL-THERM-018

227 1 9.88764316E-02 -233 234 -5 imp:n=1 u=3  
228 2 8.66829700E-02 233 -232 234 -5 imp:n=1 u=3  
c  
c fuel feed pipe 2  
c  
230 1 9.88764316E-02 -236 237 -238 imp:n=1 u=3  
231 2 8.66829700E-02 236 -235 237 -238 imp:n=1 u=3  
c  
c fuel feed pipe 3  
c  
233 1 9.88764316E-02 -241 -242 43 imp:n=1 u=3  
234 2 8.66829700E-02 241 -240 -242 43 imp:n=1 u=3  
c  
c 8 4 4.94240000E-05 #12 #163 #4 #5 #6 #7 #250 #251 #252 #253  
c #(-232 234) #(237 -238 -235) #(-242 -240) imp:n=1 u=5  
c  
c 85 0 -5 43 -51 imp:n=1 u=3 fill=5  
c  
c base plate  
13 2 8.66829700E-02 (-43 44 -45 46 -47 48) 410 imp:n=1 u=3  
330 2 8.66829700E-02 -44 412 (-45 46 -47 48) 411  
(414:-415:416:-417) imp:n=1 u=3  
331 2 8.66829700E-02 82 -413 (-45 46 -47 48) 411  
(414:-415:416:-417) imp:n=1 u=3  
332 2 8.66829700E-02 -412 413 (-418 419 -420 421) 411  
(422:-423:424:-425) imp:n=1 u=3  
333 2 8.66829700E-02 -412 413 410 -411 imp:n=1 u=3  
c neutron source guide tube  
254 4 4.94240000E-05 -531 -530 84 imp:n=1 u=3  
255 2 8.66829700E-02 531 -532 -530 84 imp:n=1 u=3  
256 4 4.94240000E-05 532 -533 -530 84 imp:n=1 u=3  
257 2 8.66829700E-02 533 -534 -530 84 imp:n=1 u=3  
86 2 8.66829700E-02 41 -42 -530 84 imp:n=1 u=3  
164 4 4.94240000E-05 534 -41 -530 84 imp:n=1 u=3  
c  
c ch-4  
21 13 5.02274000E-02 -101 -102 103 imp:n=1 u=3  
401 6 1.24933300E-01 -105 106 101 -104 imp:n=1 u=3  
c ch-5  
24 14 1.07067000E-01 -107 -108 109 imp:n=1 u=3  
410 6 1.24933300E-01 107 -110 -111 112 imp:n=1 u=3  
c ch-6  
c 27 15 8.80834000E-02 -113 -114 115 imp:n=1 u=3  
c 420 6 1.24933300E-01 113 -116 -117 118 imp:n=1 u=3  
c ch-7  
30 16 3.46630000E-02 -122 123 -119 imp:n=1 u=3  
31 16 3.46630000E-02 -122 123 119 -120 imp:n=1 u=3  
430 6 1.24933300E-01 -121 120 125 -124 imp:n=1 u=3  
c 66 4 4.94240000E-05 -121 -136 137 #30 #31 #32 imp:n=1 u=3  
c ch-1 2  
90 4 4.94240000E-05 -136 163 -180 imp:n=1 u=3  
91 7 -2.69900000E+00 -136 163 180 -161 imp:n=1 u=3  
440 6 1.24933300E-01 -162 161 163 -164 imp:n=1 u=3  
c 92 3 9.99870000E-02 -162 161 163 -164 imp:n=1 u=3  
c 93 4 4.94240000E-05 -162 -136 137 #90 #91 #92 imp:n=1 u=3  
c ch-3  
94 4 4.94240000E-05 -136 163 -190 imp:n=1 u=3  
95 7 -2.69900000E+00 -136 163 190 -181 imp:n=1 u=3  
450 6 1.24933300E-01 163 -164 181 -182 imp:n=1 u=3  
c 96 3 9.99870000E-02 -182 181 183 -184 imp:n=1 u=3  
c 97 4 4.94240000E-05 -182 -136 137 #94 #95 #96 imp:n=1 u=3  
c pulsartron  
c 33 17 2.726620E-02 -325 -126 127 imp:n=1 u=3  
c 460 6 1.249333E-01 325 -128 -129 130 imp:n=1 u=3  
c 35 3 9.99870000E-02 -128 -126 127 #33 #34 imp:n=1 u=3  
c st-a  
36 11 1.25762000E-02 -131 -134 135 imp:n=1 u=3  
37 4 4.94240000E-05 -131 -136 137 #36 imp:n=1 u=3  
38 7 -2.69900000E+00 131 -132 -136 137 imp:n=1 u=3  
470 6 1.24933300E-01 -133 132 -138 139 imp:n=1 u=3  
c 40 4 4.94240000E-05 132 -133 -136 137 #39 imp:n=1 u=3

LEU-SOL-THERM-018

```

c  st-b
41 11 1.25762000E-02 -140 -134 135      imp:n=1 u=3
42 4 4.94240000E-05 -140 -136 137 #41    imp:n=1 u=3
43 7 -2.69900000E+00 140 -141 -136 137    imp:n=1 u=3
480 6 1.24933300E-01 141 -142 -138 139    imp:n=1 u=3
c 45 4 4.94240000E-05 141 -142 -136 137 #44 imp:n=1 u=3
c  lin-a
46 12 1.86958000E-02 -143 -146 147      imp:n=1 u=3
47 4 4.94240000E-05 -143 -136 137 #46    imp:n=1 u=3
48 7 -2.69900000E+00 143 -144 -136 137    imp:n=1 u=3
49 6 1.24933300E-01 144 -145 -150 151    imp:n=1 u=3
c 50 4 4.94240000E-05 144 -145 -148 137 #49 imp:n=1 u=3
c  lin-b
51 12 1.86958000E-02 -152 -146 147      imp:n=1 u=3
52 4 4.94240000E-05 -152 -136 149 #51    imp:n=1 u=3
53 7 -2.69900000E+00 152 -153 -136 149    imp:n=1 u=3
54 6 1.24933300E-01 153 -154 -350 351    imp:n=1 u=3
c 55 4 4.94240000E-05 153 -154 -148 149 #54 imp:n=1 u=3
c  log-a
56 12 1.86958000E-02 -155 -146 147      imp:n=1 u=3
57 4 4.94240000E-05 -155 -136 149 #56    imp:n=1 u=3
58 7 -2.69900000E+00 155 -156 -136 149    imp:n=1 u=3
59 6 1.24933300E-01 156 -157 -150 151    imp:n=1 u=3
c 60 4 4.94240000E-05 156 -157 -148 149 #59 imp:n=1 u=3
c  log-b
61 12 1.86958000E-02 -158 -146 147      imp:n=1 u=3
62 4 4.94240000E-05 -158 -136 137 #61    imp:n=1 u=3
63 7 -2.69900000E+00 158 -159 -136 137    imp:n=1 u=3
64 6 1.24933300E-01 159 -160 -350 351    imp:n=1 u=3
c 65 4 4.94240000E-05 159 -160 -148 137 #64 imp:n=1 u=3
c
270 2 8.66829700E-02 3 -4 15 -16 502 -503 #(17 -18) imp:n=1 u=3
c
c  reflector support plate
c
c  Concrete reflector
c
301 21 8.11829800E-02 267 -268 272 -273 265 -266
      481 482 483 484 485 486 487 488 imp:n=1 u=3
302 22 8.68654070E-02 261 -262 272 -273 263 -264 #(267 -268 265 -266)
      imp:n=1 u=3
303 20 5.98285201E-02 261 -262 271 -274 263 -264 #(272 -273)
      481 482 483 484 485 486 487 488 imp:n=1 u=3
c
304 21 8.11829800E-02 267 -268 277 -276 265 -266
      481 482 483 484 485 486 487 488 imp:n=1 u=3
305 22 8.68654070E-02 261 -262 277 -276 263 -264 #(267 -268 265 -266)
      imp:n=1 u=3
306 20 5.98285201E-02 261 -262 278 -275 263 -264 #(277 -276)
      481 482 483 484 485 486 487 488 imp:n=1 u=3
c
307 21 8.11829800E-02 267 -268 282 -283 265 -266
      461 462 463 464 465 466 467 468
      481 482 483 484 485 486 487 488 imp:n=1 u=3
308 22 8.68654070E-02 261 -262 282 -283 263 -264 #(267 -268 265 -266)
      461 462 463 464 465 466 467 468 imp:n=1 u=3
309 20 5.98285201E-02 261 -262 281 -284 263 -264 #(282 -283)
      481 482 483 484 485 486 487 488 imp:n=1 u=3
c
310 21 8.11829800E-02 267 -268 287 -286 265 -266
      471 472 473 474 475 476 477 478
      481 482 483 484 485 486 487 488 imp:n=1 u=3
311 22 8.68654070E-02 261 -262 287 -286 263 -264 #(267 -268 265 -266)
      471 472 473 474 475 476 477 478 imp:n=1 u=3
312 20 5.98285201E-02 261 -262 288 -285 263 -264 #(287 -286)
      481 482 483 484 485 486 487 488 imp:n=1 u=3
c
c  gold wir and detector
c
313 4 4.94240000E-05 261 -262 263 -264
      (-461:-462:-463:-464:-465:-466:-467:-468)

```

LEU-SOL-THERM-018

```

                                imp:n=1 u=3
314 4 4.94240000E-05 261 -262 263 -264
      (-471:-472:-473:-474:-475:-476:-477:-478)
                                imp:n=1 u=3
315 4 4.94240000E-05 ((271 -274):(-275 278):(281 -284):(-285 288))
      (-481:-482:-483:-484:-485:-486:-487:-488)
                                imp:n=1 u=3

c
c Support of reflector
c
320 22 8.68654070E-02 (-267 261 272 -283 -263 82 ) :
      (267 -343 272 -283 -340 82 ) :
      (-267 261 272 -283 264 -342) imp:n=1 u=3
321 22 8.68654070E-02 (268 -262 272 -283 -263 82 ) :
      (-268 344 272 -283 -340 82 ) :
      (268 -262 272 -283 264 -342) imp:n=1 u=3
322 22 8.68654070E-02 (-267 261 -276 287 -263 43 ) :
      (267 -343 -276 287 -341 43 ) :
      (-267 261 -276 287 264 -342) imp:n=1 u=3
323 22 8.68654070E-02 (268 -262 -276 287 -263 43 ) :
      (-268 344 -276 287 -341 43 ) :
      (268 -262 -276 287 264 -342) imp:n=1 u=3

c
199 4 4.94240000E-05 #79 #(-42 84 -530) #13
      #270
      #21 #401 #24 #410
      #(-120 -122 123) #430 #(-136 163 -161) #440 #(-136 163 -181) #450
      #(-132 -136 137) #470 #(-141 -136 137) #480 #(-144 -136 137) #49
      #(-153 -136 149) #54
      #(-156 -136 149) #59
      #(-159 -136 137) #64
      #4 #5
      #(-232 234 -5) #(237 -238 -235) #(-242 -240 43)
      #(261 -262 271 -274 263 -264) #(261 -262 -275 278 263 -264)
      #(261 -262 281 -284 263 -264) #(261 -262 -285 288 263 -264)
      #320 #321 #322 #323
      #330 #331 #332 #333
      imp:n=1 u=3
200 0 -81 82 -83 84 -85 86 imp:n=1 u=4 fill=3
201 2 8.66829700E-02 #200 imp:n=1 u=4
202 0 -91 92 -93 94 -95 96 imp:n=1 u=6 fill=4
281 19 1.37809E-01 91 -331 -335 imp:n=1 u=6
282 2 8.66829700E-02 91 331 -171 -335 imp:n=1 u=6
283 19 1.37809E-01 91 -332 -335 imp:n=1 u=6
284 2 8.66829700E-02 91 332 -172 -335 imp:n=1 u=6
285 19 1.37809E-01 91 -333 -335 imp:n=1 u=6
286 2 8.66829700E-02 91 333 -173 -335 imp:n=1 u=6
203 0 #281 #282 #283 #284 #285 #286 #202 imp:n=1 u=6
204 0 300 -301 302 -303 304 -305 imp:n=1 u=7 fill=6
205 2 8.66829700E-02 #204 imp:n=1 u=7
206 0 306 -307 308 -309 310 -311 imp:n=1 u=8 fill=7
207 0 #206 imp:n=1 u=8
208 0 312 -313 314 -315 316 -317 imp:n=1 u=9 fill=8
209 18 8.153E-2 #208 imp:n=1 u=9
212 0 318 -319 320 -321 322 -323 imp:n=1 fill=9
211 0 #212 imp:n=0

c
c surface cards (origin x=0.0 y=0.0 z=0.0)
c cylinder
500 pz -0.0001
501 pz -1.9999
502 py -44.0
503 py 44.0
1 pz 0.0
2 pz 65.56
3 pz 149.75
4 pz 152.63
5 pz -2.04
11 px -14.04
12 px 14.04

```

LEU-SOL-THERM-018

13 py -34.515  
14 py 34.515  
15 px -16.57  
16 px 16.57  
17 py -37.045  
18 py 37.045  
c  
41 c/x -8.0 -10.0 3.905  
42 c/x -8.0 -10.0 4.455  
531 c/x -8.0 -10.0 1.3  
532 c/x -8.0 -10.0 1.5  
533 c/x -8.0 -10.0 2.65  
534 c/x -8.0 -10.0 3.0  
530 px 220.0  
c 41 gq 0.5 0.5 1. -1. 0. 0. 11.31371 -11.31371 20. 148.750975  
c 42 gq 0.5 0.5 1. -1. 0. 0. 11.31371 -11.31371 20. 144.152975  
43 pz -16.0  
44 pz -19.0  
45 py 50.0  
46 py -50.0  
47 px 17.0  
48 px -83.0  
c 49 py 78.48  
c 50 px -71.42  
c base plate lower pipe and hari  
410 c/z 2.0 17.0 7.76  
411 c/z 2.0 17.0 8.26  
412 pz -20.0  
413 pz -34.0  
414 px 2.0  
415 px -68.0  
416 py 35.0  
417 py -35.0  
418 px 9.85  
419 px -75.85  
420 py 42.85  
421 py -42.85  
422 px 9.15  
423 px -75.15  
424 py 42.15  
425 py -42.15  
c  
c foot of tank  
51 py 33.5  
52 py 34.5  
53 py 42.5  
54 py -33.5  
55 py -34.5  
56 py -42.5  
57 pz -15.0  
c  
c pool wall  
81 pz 205.4  
82 pz -35.0  
83 px 283.0  
84 px -119.0  
85 py 100.0  
86 py -100.0  
91 pz 205.401  
92 pz -36.5  
93 px 284.0  
94 px -120.0  
95 py 101.0  
96 py -101.0  
c  
c neutron counter  
c ch-4  
101 c/z 47.3 -1.0 1.85  
102 pz 63.781  
103 pz 16.381  
104 c/z 47.3 -1.0 2.85

LEU-SOL-THERM-018

105 pz 55.581  
106 pz 17.581  
c ch-5  
107 c/z -23.0 55.5 2.35  
108 pz 60.41  
109 pz 18.01  
110 c/z -23.0 55.5 3.35  
111 pz 54.21  
112 pz 19.21  
c ch-6  
113 c/z 73.0 27.5 2.35  
114 pz 77.91  
115 pz 24.51  
116 c/z 73.0 27.5 3.35  
117 pz 70.71  
118 pz 25.71  
c ch-7  
119 c/z 17.0 -52.5 4.499  
120 c/z 17.0 -52.5 4.5  
121 c/z 17.0 -52.5 5.5  
122 pz 69.75  
123 pz 18.65  
124 pz 57.65  
125 pz 21.65  
c ch-1 and 3  
180 c/z -4.5 -48.0 1.0  
161 c/z -4.5 -48.0 1.1  
162 c/z -4.5 -48.0 2.1  
163 pz -15.999  
164 pz 53.0  
c ch-2  
190 c/z 4.5 48.0 1.0  
181 c/z 4.5 48.0 1.1  
182 c/z 4.5 48.0 2.1  
c  
c pulsertron  
c 325 c/z 65.2 38.0 5.5  
c 126 pz 66.33  
c 127 pz 5.33  
c 128 c/z 65.2 38.0 10.5  
c 129 pz 36.53  
c 130 pz 6.53  
c st-a  
131 c/z 0.0 -56.8 1.95  
132 c/z 0.0 -56.8 2.25  
133 c/z 0.0 -56.8 3.25  
134 pz 36.393  
135 pz 2.103  
136 pz 205.5  
137 pz -34.999  
138 pz 42.535  
139 pz -2.465  
c st-b  
140 c/z 0.0 56.8 1.95  
141 c/z 0.0 56.8 2.25  
142 c/z 0.0 56.8 3.25  
c lin-a  
143 c/z 41.6 -54.5 4.7  
144 c/z 41.6 -54.5 5.0  
145 c/z 41.6 -54.5 5.5  
146 pz 57.445  
147 pz 12.69  
148 pz 205.5  
149 pz -15.999  
150 pz 61.28  
151 pz 5.28  
c lin-b  
152 c/z -41.6 54.5 4.7  
153 c/z -41.6 54.5 5.0  
154 c/z -41.6 54.5 5.5  
350 pz 61.28



LEU-SOL-THERM-018

351 pz 5.28  
c log-a  
155 c/z -41.6 -54.5 4.7  
156 c/z -41.6 -54.5 5.0  
157 c/z -41.6 -54.5 5.5  
c log-b  
158 c/z 41.6 54.5 4.7  
159 c/z 41.6 54.5 5.0  
160 c/z 41.6 54.5 5.5  
c  
330 pz 185.35  
335 pz 340.35  
c crd-1  
171 c/z 0.00 15.0 3.815  
221 c/z 0.00 15.0 3.095  
331 c/z 0.00 15.0 2.73  
c crd-2  
172 c/z 0.00 -15.0 3.815  
222 c/z 0.00 -15.0 3.095  
332 c/z 0.00 -15.0 2.73  
c crd-3  
173 c/z 0.0 0.0 3.815  
223 c/z 0.0 0.0 3.095  
333 c/z 0.0 0.0 2.73  
c spare  
175 c/z 10.0 30.0 3.815  
176 pz 184.5  
c n-4(level gauge)  
177 c/z -10.5 -30.0 2.4  
c n-2(gas-outlet)  
178 c/z -25.0 7.5 1.7  
c n-5(driving device)  
179 c/z -9.0 30.0 2.13  
c n-7(thermocouple guide)  
220 c/z 11.5 -25.0 1.6  
225 pz 185.0  
226 pz 5.5  
227 pz 2.5  
228 c/z 11.5 -25.0 0.865  
229 c/z 11.5 -25.0 0.545  
230 c/z 11.5 -25.0 1.475  
231 c/z 11.5 -25.0 0.975  
c  
c fuel feed pipe  
232 c/z 12.5 29.0 1.36  
233 c/z 12.5 29.0 1.07  
234 pz -9.6  
235 gq 0.5 0.5 1. -1. 0. 0. 16.5 -16.5 22. 255.275  
236 gq 0.5 0.5 1. -1. 0. 0. 16.5 -16.5 22. 255.98  
c 235 c/x 29.0 -11.0 1.36  
c 236 c/x 29.0 -11.0 1.07  
238 p 1. 1. 0. 41.5  
237 p 1. 1. 0. 19.0  
c 238 px 12.5  
c 237 px -12.5  
c 239 px 6.2  
240 c/z 2.0 17.0 1.36  
241 c/z 2.0 17.0 1.07  
242 pz -12.3601  
c  
c Reflector support plate  
c  
c Kirikaki  
c  
378 p 1. -1. 0. -51.33595  
379 p 1. -1. 0. 51.33595  
380 p 1. 1. 0. 51.33595  
381 p 1. 1. 0. -51.33595  
382 p 1. -1. 0. -12.02082  
383 p 1. -1. 0. 12.02082  
384 p 1. 1. 0. 12.02082

Revision: 0

Date: September 30, 2001

LEU-SOL-THERM-018

385 p 1. 1. 0. -12.02082

c c150+C50 concrete reflector

c

261 py -38.7

262 py 38.7

263 pz -3.0

264 pz 153.6

265 pz 0.0

266 pz 150.6

267 py -35.7

268 py 35.7

271 px 16.79

272 px 17.60

273 px 22.61

274 px 23.42

275 px -16.79

276 px -17.60

277 px -22.61

278 px -23.42

281 px 23.50

282 px 24.31

283 px 39.31

284 px 40.12

285 px -23.50

286 px -24.31

287 px -39.31

288 px -40.12

c c150+C50 detector and gold wire

c

461 c/z 35.31 8.0 0.25

462 c/z 35.31 -8.0 0.25

463 c/z 35.31 22.0 0.8

464 c/z 35.31 -22.0 0.8

465 c/z 27.31 8.0 0.8

466 c/z 27.31 -8.0 0.8

467 c/y 31.81 20.0 0.8

468 c/y 31.81 70.0 0.8

c

471 c/z -35.31 8.0 0.25

472 c/z -35.31 -8.0 0.25

473 c/z -35.31 22.0 0.8

474 c/z -35.31 -22.0 0.8

475 c/z -27.31 8.0 0.8

476 c/z -27.31 -8.0 0.8

477 c/y -31.81 20.0 0.8

478 c/y -31.81 70.0 0.8

c

481 c/x 15.0 30.0 0.25

482 c/x 15.0 60.0 0.25

483 c/x 15.0 90.0 0.25

484 c/x -15.0 30.0 0.25

485 c/x -15.0 60.0 0.25

486 c/x -15.0 90.0 0.25

487 c/x 0.0 30.0 0.8

488 c/x 0.0 60.0 0.8

c

c Reflector support

c

340 pz -33.0

341 pz -14.0

342 pz 170.5

343 py -24.5

344 py 24.5

c

c Hood and Concrete

c

300 px -487.5

301 px 512.5

302 py -290.0

303 py 610.0

304 pz -290.0

LEU-SOL-THERM-018

305 pz 738.0  
306 px -488.2  
307 px 513.2  
308 py -290.7  
309 py 610.7  
310 pz -290.7  
311 pz 738.7  
312 px -617.0  
313 px 642.0  
314 py -400.0  
315 py 910.0  
316 pz -295.0  
317 pz 915.0  
318 px -797.0  
319 px 842.0  
320 py -610.0  
321 py 1090.0  
322 pz -395.0  
323 pz 1065.0

c  
c data cards  
c  
mode n \$ transport neutrons only  
c  
c material cards  
c  
c R145(C200);U=313.8/A=0.955/D=1.4500  
c atomic density = 9.88764316E-02  
m1 1001.37c 5.8747E-02  
7014.37c 2.1648E-03  
8016.37c 3.7170E-02  
92234.37c 6.4595E-07  
92235.37c 8.0158E-05  
92236.37c 8.0058E-08  
92238.37c 7.1398E-04  
mt1 lwtr.01t \$ 300k  
c  
c sus304L(tank) 7.93g/cm3  
c atomic density 8.668297E-2  
m2 6012.37c 7.1567E-05 \$ C  
14000.37c 7.1415E-04 \$ Si  
25055.37c 9.9095E-04 \$ Mn  
15031.37c 5.0879E-05 \$ P  
16000.37c 1.0424E-05 \$ S  
28000.37c 8.5600E-03 \$ Ni  
24000.37c 1.6725E-02 \$ Cr  
26000.37c 5.9560E-02 \$ Fe  
c  
c water 25 deg.c  
c  
m3 1001.37c 6.6658E-02 \$ H  
8016.37c 3.3329E-02 \$ O  
mt3 lwtr.01t \$ 300K  
c  
c air  
c  
m4 7014.37c 3.9014E-05  
8016.37c 1.0410E-05  
c  
c polyethylene 0.97g/cm3  
m6 1001.37c 8.32889E-02  
6012.37c 4.16444E-02  
mt6 poly.01t \$ 300k  
c  
c aluminum 2.699g/cm3  
m7 13027.37c -100.0 \$ Al  
c  
c sus304 7.93g/cm3 (d)daiza,annaikan etc.  
m9 6012.37c -0.05 \$ C  
14000.37c -0.41 \$ Si

Revision: 0

Date: September 30, 2001

LEU-SOL-THERM-018

25055.37c -0.93 \$ Mn  
15031.37c -0.030 \$ P  
16000.37c -0.004 \$ S  
28000.37c -8.29 \$ Ni  
24000.37c -18.36 \$ Cr  
26000.37c -71.930 \$ Fe

c  
c st-a,b (1.25762e-2)  
m11 6012.37c 1.51491E-7 \$ C  
8016.37c 3.02982E-7 \$ O  
13027.37c 1.25729E-2 \$ Al  
18040.37c 2.85066E-6 \$ Ar

c  
c lin-a,b,log-a,b (1.86958e-2)  
m12 7014.37c 3.82159E-5 \$ N  
13027.37c 1.86576E-2 \$ Al

c  
c ch-4(wl) (5.02274e-2)  
m13 6012.37c 8.92716E-8 \$ C  
8016.37c 1.78543E-7 \$ O  
13027.37c 5.02254E-2 \$ Al  
18040.37c 1.70771E-6 \$ Ar

c  
c ch-5 (1.07067e-1)  
m14 7014.37c 3.11542E-5 \$ N  
13027.37c 1.07036E-1 \$ Al

c  
c ch-6 (8.80834e-2)  
m15 7014.37c 2.47374E-5 \$ N  
13027.37c 8.80587E-2 \$ Al

c  
c ch-7 (3.46630e-2)  
m16 7014.37c 2.27114E-5 \$ N  
13027.37c 3.46403E-2 \$ Al

c pulsartron  
m17 6012.37c 3.54473E-5 \$ C  
13027.37c 1.29223E-2 \$ Al  
14000.37c 1.14537E-4 \$ Si  
25055.37c 1.33181E-4 \$ Mn  
15031.37c 7.73834E-6 \$ P  
16000.37c 8.85058E-7 \$ S  
28000.37c 1.11341E-3 \$ Ni  
24000.37c 2.78370E-3 \$ Cr  
26000.37c 1.01550E-2 \$ Fe

c HANDBOOK Concrete  
m18 1001.37c 1.3742e-2 \$ H  
8016.37c 4.5919e-2 \$ O  
6012.37c 1.1532e-4 \$ C  
11023.37c 9.6395e-4 \$ Na  
12000.37c 1.2388e-4 \$ Mg  
13027.37c 1.7409e-3 \$ Al  
14000.37c 1.6617e-2 \$ Si  
19000.37c 4.6052e-4 \$ K  
20000.37c 1.5025e-3 \$ Ca  
26000.37c 3.4492e-4 \$ Fe

mt18 lwtr.01t  
c  
c B4C (2.51g/cm3)  
c 1.37809e-1  
m19 5010.37c 2.18289e-2  
5011.37c 8.84185e-2  
6012.37c 2.75619e-2

c  
c Aluminum for reflector  
c atomic density 5.98285201E-02  
m20 13027.37c 5.9559E-02 \$ Al  
14000.37c 8.0751E-05 \$ Si  
26000.37c 1.7114E-04 \$ Fe  
29000.37c 1.7845E-05 \$ Cu

c  
c concrete (STACY-280T) T-ave.  
c atomic density 8.11829800E-02

LEU-SOL-THERM-018

```

m21 1001.37c 1.4528e-02
      8016.37c 4.4590E-02
      11023.37c 1.0533E-03
      12000.37c 1.9573E-04
      13027.37c 1.5533E-03
      14000.37c 1.4749E-02
      16000.37c 1.0906E-04
      17000.37c 9.0027E-07
      19000.37c 1.9179E-04
      20000.37c 3.9337E-03
      26000.37c 2.7830E-04
mt21 lwtr.01t
c
c sus304L(futa) 7.93g/cm3
c atomic density 8.68654070e-02
m22 6012.37c 2.0675E-04 $ C
      14000.37c 6.6314E-04 $ Si
      25055.37c 1.0083E-03 $ Mn
      15031.37c 4.9337E-05 $ P
      16000.37c 1.6380E-05 $ S
      28000.37c 6.6885E-03 $ Ni
      24000.37c 1.6798E-02 $ Cr
      26000.37c 6.1435E-02 $ Fe
c
c sus304 Kadai
m23 6012.37c 1.5904E-04 $ C
      14000.37c 9.3519E-04 $ Si
      25055.37c 1.1213E-03 $ Mn
      15031.37c 4.4712E-05 $ P
      16000.37c 2.9782E-06 $ S
      28000.37c 6.8512E-03 $ Ni
      24000.37c 1.6890E-02 $ Cr
      26000.37c 6.0951E-02 $ Fe
c
c criticality cards
c
kcode 5000 1.0 50 2050
sdef cel=d1 x=d2 y=d3 z=d4 erg=d5
c
si1 1 212:208:206:204:202:200:79:1
sp1 1
c *** x-coordinate
si2 h -14.0 14.0
sp2 0 1
c *** y-coordinate
si3 h -34.5 34.5
sp3 0 1
c *** z-coordinate
si4 h 0.0 65.56
sp4 0 1
c
sp5 -3
c
c ctme 25
prdmp j -100 1 3
c
print -175

```

**APPENDIX F: DERIVATION OF ATOM DENSITIES OF FUEL SOLUTION****Run No.145 (C200 Reflector)**

|   |   |
|---|---|
| Atomic weight of H=                     | A1= 1.0079  |
| Atomic weight of N=                     | A7= 14.0067   |
| Atomic weight of O=                     | A8= 15.9994   |
| Atomic weight of U234=                  | A24= 234.0409   |
| Atomic weight of U235=                  | A25= 235.0439   |
| Atomic weight of U236=                  | A26= 236.0456   |
| Atomic weight of U238=                  | A28= 238.0508   |
| Wt.% of U234=                           | W24= 0.08   |
| Wt.% of U235=                           | W25= 9.97   |
| Wt.% of U236=                           | W26= 0.01   |
| Wt.% of U238=                           | W28= 89.94  |
| Uranium concentration (g/l)=            | UD= 313.8   |
| Free nitric acid concentration (mol/l)= | AC= 0.955   |
| Solution density (g/cc)=                | D= 1.4500   |
| Avogadro's number=                      | AV= 0.60221   |
| Atom density of U234=N24=               | UD/1000*W24/100/A24*AV= 6.4595E-07                          |
| Atom density of U235=N25=               | UD/1000*W25/100/A25*AV= 8.0158E-05                          |
| Atom density of U236=N26=               | UD/1000*W26/100/A26*AV= 8.0058E-08                          |
| Atom density of U238=N28=               | UD/1000*W28/100/A28*AV= 7.1398E-04                          |
| Total uranium atom density=             | UN= 7.9486E-04  |
| HNO3                                    |   |
| NH(HNO3)=                               | AC/1000*AV= 5.7511E-04                                      |
| NN(HNO3)=                               | AC/1000*AV= 5.7511E-04                                      |
| NO(HNO3)=                               | AC/1000*AV*3= 1.7253E-03                                    |
| Density of HNO3 (g/cc)=DN=              | AC*(A1+A7+3*A8)/1000= 0.060177224                           |
| UO2(NO3)2                               |   |
| Molecular weight of UO2(NO3)2=MWU=      | (N24*A24+N25*A25+N26*A26+N28*A28)/UN+2*A7+8*A8= 393.7527074 |
| Density of UO2(NO3)2=DU=                | MWU*UN/AV= 0.51971677                                       |
| Density of H2O=DH=                      | D-DU-DN= 0.870106006  |
| NH(H2O)=                                | DH/(2*A1+A8)*AV*2= 5.8172E-02                               |
| NO(H2O)=                                | DH/(2*A1+A8)*AV= 2.9086E-02                                 |
| Atom density of H=                      | NH(HNO3)+NH(H2O)= 5.8747E-02                                |
| Atom density of O=                      | NO(H2O)+NO(HNO3)+8*UN= 3.7170E-02                           |
| Atom density of N=                      | NN(HNO3)+2*UN= 2.1648E-03                                   |